Molecular Orbital Modeling and Transition State Theory in Geochemistry

Article *in* Reviews in Mineralogy and Geochemistry · January 2001

DOI: 10.2138/rmg.2001.42.14

3 authors:

Mihali Felipe
Yale University
8 PUBLICATIONS **93** CITATIONS
SEE PROFILE

Yitian Xiao
ExxonMobil
42 PUBLICATIONS **1,307** CITATIONS
SEE PROFILE

J. D. Kubicki
University of Texas at El Paso
259 PUBLICATIONS **8,333** CITATIONS
SEE PROFILE

14 Molecular Orbital Modeling and Transition State Theory in Geochemistry

Mihali A. Felipe
Department of Geology and Geophysics
Yale University
New Haven, Connecticut, 06511, U.S.A.

Yitian Xiao
ExxonMobil Upstream Research Company
3319 Mercer Street
Houston, Texas, 77027-6019, U.S.A.

James D. Kubicki
Department of Geosciences
The Pennsylvania State University
University Park, Pennsylvania, 16802, U.S.A.

INTRODUCTION

Fundamental to the understanding of geochemical phenomena is the accurate determination of viable chemical reactions and their rates. The accurate determination of the rate constants of underlying chemical reaction are needed by numerous other areas of science and engineering as well, and it is no coincidence that predicting rate constants has become a major goal of computational chemistry. In this chapter, we discuss the possible determination of these rate constants and mechanisms in the geosciences through molecular orbital (MO) calculations and transition state theory.

The rate constants and their temperature dependence are critical in geochemical kinetics. Knowledge of the temperature dependent rates allows the computation of reaction progress over a range of temperatures. Furthermore, if the forward and backward rate constants k_f and k_r are known for an elementary reaction, then the equilibrium constant K_{eq} for that elementary reaction can be calculated as well, for

$$K_{eq}(T) = k_f(T)/k_b(T) \tag{1}$$

where (T) is used to emphasize the temperature dependence. Note that this enables the direct computation of the equilibrium isotope fractionation factors for overall reactions. In addition to knowing the rates of the reactions *per se* and calculating equilibrium constants for elementary reactions, knowledge of the thermal rate constants allows the prediction of phenomena such as kinetic isotope effects (KIE). For instance, the primary kinetic isotope effect of an elementary reaction may be evaluated using

$$\mathrm{KIE}(T) = k_f^*(T)/k_f(T) \tag{2}$$

assuming that the isotope is directly involved in the reaction and where the asterisk indicates the same reaction but with a different isotopic signature.

Conventional transition state theory (TST) provides a formalism for predicting thermal rate constants by combining the important features of the potential energy surface (PES) with a statistical representation of the dynamics of the system. MO calculations, on the other hand, allow the numerical determination of the PES. Thus, MO theory used in

1529-6466/00/0042-0014$05.00

conjunction with TST provides a means by which the reactive properties of molecules may be quantified with varying degrees of independence from empirical methods. First principles or *ab initio* methods, which are by definition free from experimental data (except for fundamental physical constants such as the charge of an electron and nuclear masses), represent one end-member of these calculations. We shall use the term MO-TST to mean the use of MO data in the framework of TST to elucidate reaction kinetics.

A PES may also be generated using empirically-derived molecular force fields. These "empirical" methods are less computationally expensive than MO calculations, allowing the application to larger systems. However, force fields or molecular mechanics calculations are in general not applicable to the determination of the crucial features of the PES that are necessary for the calculation of thermal rate constants using TST. In reactions where there are bond-breaking and bond-forming steps, force fields may not be accurate because they are typically parameterizing for near-equilibrium structures. Solving this inadequacy has been the focus of recent efforts to develop newer reactive force fields that will elucidate these features of the PES (see Gale and Parker et al. chapters, this volume; Demiralp 1999). Such force fields developments could benefit from the use of MO calculations to provide the necessary energy versus structure information for configurations far from equilibrium. We will confine our discussion mainly to *ab initio* methods in this chapter.

The need for a means of obtaining reactivity properties of molecules with varying independence from experiment may be appreciated when one realizes that there are systems wherein MO calculations may be the only method available for analysis. For example, the determination of elementary reaction steps in complex overall geochemical reactions such as dissolution may be a daunting problem even for the most experienced experimentalist. MO calculations can help in elucidating reaction mechanisms and energetics when these are obscure, difficult to determine, or simply unexplored. Improvements in MO calculations have increased the accuracy and cost effectiveness of modeling relative to experiments and have led researchers to use MO-TST to predict reaction paths as an aid to understanding experimental results.

TRANSITION STATE THEORY

Conventional transition state theory

Formalism. The theory was introduced by Eyring (1935a,b) and has been a powerful concept in the study of chemical reaction kinetics. Since this introduction, numerous excellent texts have been written about the subject (Glasstone et al. 1941; Pechukas 1976; Truhlar et al. 1983, 1996) that may be consulted for a more rigorous or thorough coverage. Lasaga (1981, 1998) has excellent discussions of TST in the geosciences. We review the salient points of the theory below.

One of the fundamental assumptions of TST is that there exists a divide in the PES that separates the reactant and product regions. This divide contains the transition state, which is defined as the maximum value on the minimum energy path of the PES that connects reactant(s) and product(s). Any trajectory passing through the divide from the reactant side is assumed to form products eventually; this is often referred to the as the "non-recrossing rule." Consider the generalized elementary gas phase abstraction reaction

$$XY + Z \overset{K^{\ddagger}}{\Leftrightarrow} XYZ^{\ddagger} \rightarrow X + YZ \qquad (3)$$

Figure 1 shows the PES for the collinear-only H=X=Y=Z reaction path. If τ is defined to be the average lifetime of the transition state, and each transition state complex is

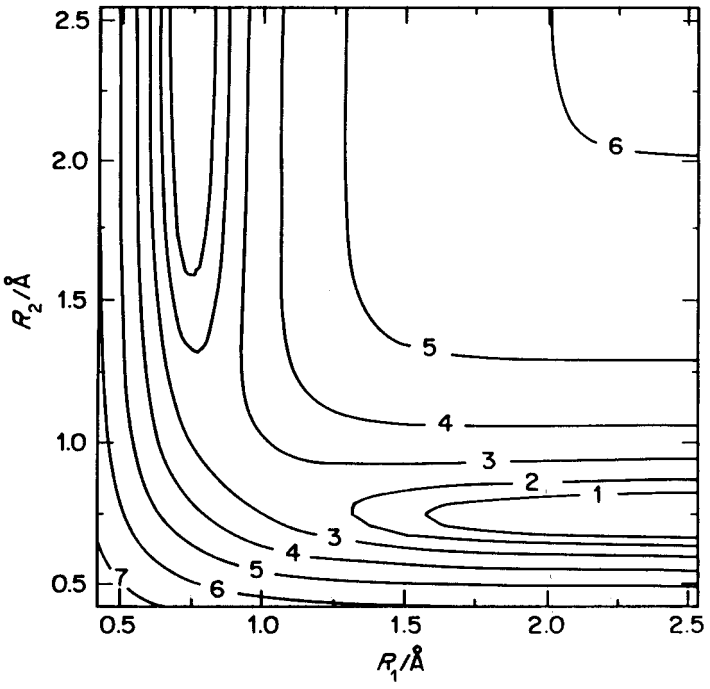

Figure 1. PES contour map of the collinear-only H-H-H reaction based on the London-Eyring-Polyani-Sato function or LEPS (See Murrell et al. 1984). R_1 and R_2 correspond to the two bond distances. [Used by permission of © John Wiley & Sons Ltd., from Murrell et al. (1984), *Molecular Potential Energy Functions*, Fig. 8.1, p. 109].

assumed to turn to products, then the concentration change per unit time of the particles moving to the right of the reaction is

$$Rate = \frac{[\mathrm{XYZ}^{\ddagger}]}{\tau} \tag{4}$$

Assuming equilibrium between reactants and the activated complexes, the rate for Equation 3 may also be represented by

$$Rate = k_r(T)[\mathrm{XY}][\mathrm{Z}] \tag{5}$$

Solving for $k_r(T)$ using Equations (4) and (5), and assuming for simplicity an ideal system, gives

$$k_r(T) = \frac{[\mathrm{XYZ}^{\ddagger}]}{\tau[\mathrm{XY}][\mathrm{Z}]} = \frac{K^{\ddagger}(T)}{\tau} = \nu^{\ddagger}(T)K^{\ddagger}(T) \tag{6}$$

where $\nu^{\ddagger} = 1/\tau$ is the unimolecular frequency of conversion of $\mathrm{XYZ}^{\ddagger}$ to products. The assumption that the reactant(s) and activated complex are in equilibrium with each other leads to the formulation of a quasi-equilibrium constant $K^{\ddagger}(T)$. The equilibrium assumption also leads to the use of quasi-thermodynamic extensive variables that are treated as if they were true thermodynamic values.

If all species are treated as ideal gases and the quasi-equilibrium constant is represented in terms of molecular partition functions q_i, we obtain (McQuarrie 1973)

$$K^{\ddagger}(T) = \frac{\left(q_{XYZ^{\ddagger}}/V\right)}{\left(q_{XY}/V\right)\left(q_Z/V\right)} e^{\frac{-\Delta\varepsilon_o}{kT}} \tag{7}$$

where V is the volume. Here, the partition functions are referenced to the PES from the zero-point energies (ZPE = $^1/_2\Sigma h\nu$ where ν is a vibrational frequency) and $\Delta\varepsilon_o$ is the difference in zero-point energies between the reactant and the transition state. Reactants and transition states are energy minima of the PES and first-order saddle points of the PES, respectively. A first-order saddle point has all but one positive second derivative. Therefore, $q_{XYZ^\ddagger}$ has a component of an imaginary vibrational mode (i.e., the negative second derivative) that can be considered a translational mode. The imaginary vibrational mode can be separated out by

$$q_{XYZ^\ddagger} = q^{\updownarrow} q_{transl} \tag{8}$$

where $q^{\updownarrow}$ involves the same total partition function of $XYZ^\ddagger$ but without the imaginary vibration which is treated as a translation, q_{transl}. Then, the rate constant can be expressed as

$$k_r = \frac{\nu^\ddagger q_{transl}\left(q^{\updownarrow}/V\right)}{\left(q_{XY}/V\right)\left(q_Z/V\right)} e^{\frac{-\Delta\varepsilon_o}{kT}} \tag{9}$$

There are various expressions for $\nu^\ddagger$ and q_{transl}, but in any proper derivation, one gets

$$\nu^\ddagger q_{transl} = \frac{kT}{h} \tag{10}$$

Therefore,

$$k_r = \frac{kT}{h} \frac{\left(q^{\updownarrow}/V\right)}{\left(q_{XY}/V\right)\left(q_Z/V\right)} e^{\frac{-\Delta\varepsilon_o}{kT}} \tag{11}$$

An analogous derivation can be given for the general case leading to

$$k_r = \frac{kT}{h} \frac{Q^{\updownarrow}}{Q_R} e^{\frac{-\Delta\varepsilon_o}{kT}} \tag{12}$$

where we have used full partition functions Q_i. We will refer to either of Equations (11) or (12) as the "rate constant equation." The significance of these relationships is that we are able to compute the rate constants of a given elementary reaction if we know the zero-point energies and the partition functions of the reactants and the transition state.

TST was originally formulated for use in the gas phase although its use has been extended to condensed phases as well (Truhlar et al. 1996). Hynes (1985) has an excellent discussion covering condensed states. In contrast to gas-phase reactions where the reaction is driven by well-defined collisions, reactions in condensed phases should consider the environment of the reaction complex (Fig. 2). The rate constants calculated for reactions in the liquid phase are valid if the transfer of energy into the system and the transport of reactants into the reaction zone are not rate limiting. In the solid state, the environment is more defined and TST has even been used to study the spatial diffusion of reactants (Doll and Voter 1987).

Partition functions. If in addition to the ideal gas assumption above, we suppose that the species can be approximated by a rigid rotor-harmonic oscillator treatment, then the molecular partition function of a species i may be separated into its molecular

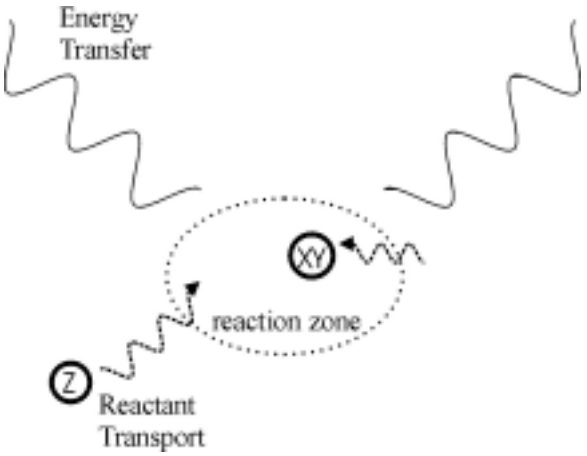

Figure 2. Schematic of reaction XY + Z → X + YZ in condensed phase showing energy transfer into the system and reactant transport to the "reaction zone." The computed rate constant would be valid if neither the energy transfer nor the reactant transport is rate limiting.

translational, rotational, vibrational, electronic and nuclear partition functions

$$q_i = q_{i,transl} q_{i,rot} q_{i,vib} q_{i,elec} q_{i,nuc} \tag{13}$$

(There are some exceptions to this separation, for instance in cases where the rotational and electronic angular momenta are coupled, but it is generally valid as a useful approximation. See Herzberg 1950.) This separation is convenient because the form of each partition function has been derived (McQuarrie 1973; Davidson 1962).

We examine each of these partition functions considering polyatomic molecules as the general case. The translational partition function is given by

$$q_{i,transl} = \left(\frac{2\pi mkT}{h^2} \right)^{3/2} V \tag{14}$$

The only data needed for the translation partition function is the mass m of i. We notice that the quantity V in the rate constant equation need not be known because it is eventually canceled by the translational partition function.

The rotational partition function depends on the shape of the molecule. For a linear polyatomic molecule, it is given by

$$q_{i,rot} = \left(\frac{8\pi^2 IkT}{\sigma h^2} \right) \tag{15}$$

where I is the moment of inertia and σ is the symmetry number, which is the number of different ways the molecule can be rotated into a configuration indistinguishable from the original (including the 1-fold rotation). For a non-linear polyatomic molecule, the partition function is given by

$$q_{i,rot} = \frac{\pi^{1/2}}{\sigma} \left(\frac{8\pi^2 I_x kT}{h^2} \right)^{1/2} \left(\frac{8\pi^2 I_y kT}{h^2} \right)^{1/2} \left(\frac{8\pi^2 I_z kT}{h^2} \right)^{1/2} \tag{16}$$

where I_k are the three principal moments of inertia corresponding to the three principal rotational modes. The moment of inertia, and the principal moments of inertia, are all functions of the atomic coordinates and their masses

$$I = I(m_1, \mathbf{r}_1, m_2, \mathbf{r}_2, \ldots) \tag{17}$$

Therefore, the rotational partition function requires knowledge only of the configuration of i and the masses m_i of the constituent atoms.

The vibrational partition function relative to the ZPE is a function of the vibrational frequencies ν for each vibrational mode j,

$$q_{i,vib} = \prod_{j=1}^{\alpha} \frac{1}{(1-e^{-h\nu_j/kT})} \tag{18}$$

Therefore, in addition to knowledge of the configuration of i, $q_{i,vib}$ requires an analysis of the second derivatives to provide vibrational frequencies (see Kubicki, this volume) of the PES in the vicinity of the reactants, products and transition state complex.

The nuclear partition function is a Boltzmann-weighted sum of the degeneracy of each nuclear state. In general, only the first term is relevant because the energy differences between the states are extremely large and transitions between the different states does not normally occur in chemical reactions

$$q_{i,nuc} = \sum \omega_{nj} e^{\frac{-\varepsilon_{nj}}{kT}} = \omega_{n1} e^{\frac{-\varepsilon_{n1}}{kT}} \tag{19}$$

where ω_{nj} is the degeneracy of the nuclear state j and ε_{nj} is the corresponding nuclear energy. If the nuclear ground state is used as reference, ε_{n1}=0, then the $q_{i,nuc}$ only contributes a multiplicative constant to q_i, specifically ω_{nj}. Because the nuclear states in general do not change as the system goes from reactants to transition state, we assume $q_{i,nuc}$ is unity in Equation (19).

Similar to the nuclear partition function, the electronic partition function is a Boltzmann-weighted sum of the degeneracy of each electronic state

$$q_{i,elec} = \sum \omega_{ej} e^{\frac{-\varepsilon_{ej}}{kT}} \tag{20}$$

where ω_{ej} is the degeneracy of the electronic state j and ε_{ej} is the corresponding electronic energy. The first term involves the electronic ground state energy (j=0) and the succeeding terms are excited energy levels; these energies can be computed by MO calculations. The electronic ground state energy is part of the solution of the PES as we shall later see.

In summary, we have shown that a number of parameters are required to evaluate the partition functions needed in the rate constant equation. Specifically, the following are needed: (1) the masses of the constituent atoms; (2) the configuration; and lastly (3) the PES in the vicinity of the configuration. The first one of these is trivial, the last two are critical and are what MO calculations provide. In the following subsection, we briefly discuss the computation of the PES; we forgo a discussion of determining reactant and product configurations and assume they have been determined. (See Cygan, this volume, and Gale, this volume, for a discussion of energy minimizations.) The determination of the transition state complex configurations is discussed in the section "Determination of Elementary Steps and Reaction Mechanisms."

Potential energy surfaces and MO calculations

We have made use of the PES in the discussion on TST without any elaboration on what a PES is. Here we define what is meant by PES, discuss how to compute the PES, and the pertinent results that may be extracted from it (e.g., the vibrational frequencies).

Assume there is a function, Ψ, called a wavefunction, which is a complete

description of the electron density of a system. $\boldsymbol{\Psi}$ defines the chemical properties of the system, so it may be assumed that $\boldsymbol{\Psi}$ is dependent on the coordinates of the electrons and the nuclei. Thus, $\boldsymbol{\Psi} = \boldsymbol{\Psi}(\mathbf{R}, \mathbf{r})$, where $\mathbf{R}$ are the coordinates for the nuclei and $\mathbf{r}$ is for the electrons. Let there be a linear operator $\mathbf{H}$ operating on $\boldsymbol{\Psi}$ in such a way that it gives the scalar value for the energy, i.e., $\mathbf{H}\boldsymbol{\Psi} = E_{tot}\boldsymbol{\Psi}$—the Schrödinger equation. This operator clearly may be further resolved into potential and kinetic energy terms. Thus,

$$\mathbf{H}\boldsymbol{\Psi} = [\mathbf{T}_n(\mathbf{R}) + \mathbf{T}_{el}(\mathbf{r}) + \mathbf{V}_{nn}(\mathbf{R}) + \mathbf{V}_{ne}(\mathbf{R},\mathbf{r}) + \mathbf{V}_{ee}(\mathbf{r})]\ \boldsymbol{\Psi} = E_{tot}\ \boldsymbol{\Psi}(\mathbf{R},\mathbf{r}) \tag{21}$$

Where $\mathbf{T}_n$ and $\mathbf{T}_{el}$ are the kinetic energy operators for the nuclei and electrons, and $\mathbf{V}_{nn}$, $\mathbf{V}_{ne}$ and $\mathbf{V}_{ee}$ are the electrostatic potential energies arising from internuclear, nucleus-electron, and interelectronic interactions. At this point, the Born-Oppenheimer approximation is invoked, i.e., the assumption that the movement of electrons is much faster than that of the nuclei and therefore the two can be decoupled from one another. This is mathematically represented by a separation of variables in the wavefunction, $\boldsymbol{\Psi}(\mathbf{R},\mathbf{r})=\boldsymbol{\Phi}(\mathbf{r}(\mathbf{R}))\ \boldsymbol{\chi}(\mathbf{R})$, where $\boldsymbol{\Phi}$ and $\boldsymbol{\chi}$ are the electronic and nuclear wavefunctions, respectively, and $\boldsymbol{\Phi}$ is a function of $\mathbf{r}$ parameterized by $\mathbf{R}$. Thus, with some rearrangement, Equation (21) becomes

$$E_{tot}\ \boldsymbol{\Phi}(\mathbf{r}(\mathbf{R}))\ \boldsymbol{\chi}(\mathbf{R}) = [\mathbf{T}_n(\mathbf{R}) + \mathbf{V}_{nn}(\mathbf{R}) + \mathbf{T}_{el}(\mathrm{r}) + \mathbf{V}_{ne}(\mathbf{R},\mathbf{r}) + \mathbf{V}_{ee}(\mathbf{r})]\ \boldsymbol{\Phi}(\mathbf{r}(\mathbf{R}))\ \boldsymbol{\chi}(\mathbf{R})$$

or

$$[T_n + V_{nn} + E_{el}]\ \boldsymbol{\Phi}(\mathbf{r}(\mathbf{R}))\ \boldsymbol{\chi}(\mathbf{R})$$
$$= \boldsymbol{\Phi}(\mathbf{r}(\mathbf{R}))\ [\mathbf{T}_n(\mathrm{R}) + \mathbf{V}_{nn}(\mathbf{R})]\ \boldsymbol{\chi}(\mathbf{R}) + \boldsymbol{\chi}(\mathbf{R})\ [\mathbf{T}_{el}(\mathbf{r}) + \mathbf{V}_{ne}(\mathbf{R},\mathbf{r}) + \mathbf{V}_{ee}(\mathbf{r})]\ \boldsymbol{\Phi}(\mathbf{r}(\mathbf{R})) \tag{22}$$

where T_n , V_{nn} , and E_{el} are the eigenvalues of $\mathbf{T}_n(\mathbf{R})$, $\mathbf{V}_{nn}(\mathbf{R})$, and $[\mathbf{T}_{el}(\mathrm{r}) + \mathbf{V}_{ne}(\mathbf{R},\mathbf{r}) + \mathbf{V}_{ee}(\mathbf{r})]$ respectively. Assuming no nuclear motion, then T_n=0. Thus wavefunction solutions to the two eigenvalue problems,

$$V_{nn}\ \boldsymbol{\chi}(\mathbf{R}) = \mathbf{V}_{nn}(\mathbf{R})\ \boldsymbol{\chi}(\mathbf{R}) \tag{23}$$

and

$$E_{el}\ \boldsymbol{\Phi}(\mathbf{r}(\mathbf{R})) = [\mathbf{T}_{el}(\mathrm{r}) + \mathbf{V}_{ne}(\mathbf{R},\mathbf{r}) + \mathbf{V}_{ee}(\mathrm{r})]\ \boldsymbol{\Phi}(\mathbf{r}(\mathbf{R})) \tag{24}$$

make a complete solution to Equation (21) within all the given assumptions. These two equations imply that the electronic energy may be solved independently from the nuclear energy.

The sum, $V_s = V_{nn} + E_{el}$, is the so-called "potential energy surface" (PES) of the system and is a function of the nuclear coordinates $\mathbf{R}$. Note that it includes the kinetic energy of the electrons and, in fact, it includes all the energy terms except for the nuclear kinetic energy $\mathbf{T}_n$. Each $\mathbf{R}$ theoretically has a computable energy in the PES but the interrelationships between the different subatomic particles make the problem impossible to solve analytically and is therefore solved numerically. Recent techniques have made it possible to arrive at satisfactory solutions. Most developments in molecular orbital methods are devoted to accurately approximating the solution to Equation (24). Hartree-Fock, Møller-Plesset, and density-functional theory are among some of the common *ab initio* methods available. Table 1 lists some of the *ab initio* and semi-empirical methods for computing the PES. Foresman and Frisch (1996) provide an excellent primer to these methods. Lately, a key thrust in quantum mechanics has been to find algorithms that linearly scale with the system size enabling large systems to be studied. The solution of

Table 1. Some *ab initio* and semi-empirical methods for computing the PES.

Methods	Availability*
Self-consistent field (SCF) methods:	
Hartree-Fock (HF)	C, GM, G98, J, MC, MO, NW
Multi-configuration active space (MCSCF)	GM, MO, NW
Complete active space SCF (CASSCF)	G98, MO, NW
Generalized valence bond (GVB)	G98, GM, J
Complete active space GVB (CASGVB)	MO
Full CI	G98, GM, MO
Post-SCF methods:	
Moller-Plesset perturbation theory (MP)	C, G98, GM, J, MO, NW
Configuration interaction (CI)	C, GM, G98, J, MC, MO, NW
Quadratic CI (QCI)	C, G98, MO
Coupled cluster (CC)	C, G98, MO, NW
Brueckner doubles (BD)	G98, MO
Outer valence Green's function (OVGF)	G98
Density Functional Methods (DFT):	
Exchange:	
Slater Local spin density (LSD) exchange	C, G98, J, MO, NW
x-alpha exchange	G98, J
Becke 1988 exchange (B)	C, G98, J, MO
Correlation:	
Vosko-Wilk-Nusair correlation (VWN)	G98, J, MO, NW
Vosko-Wilk-Nusair functional 5 (VWN V)	G98, J
Lee, Yang and Parr correlation (LYP)	C, G98, J, MO
Perdew 1981, 1986 correlations	C, G98, J, MO
Perdew-Wang correlation (PW)	C, G98, J
Perdew-Zunger correlation (PZ)	J
Colle-Salvetti correlation (CS)	MO
Hybrids:	
Becke half and half	J
Becke 1 and 3-parameter hybrids (B3-)	C, G98, J
High Accuracy Energies:	
Gaussian 1 and 2 theories (G1 and G2)	G98
Complete basis set methods (CBS)	G98
Excited State Calculations	G98, MC
Semi-empirical:	
Complete neglect of differential overlap (CNDO)	G98
Intermediate neglect of differential overlap (INDO)	G98
Modified INDO (MINDO)/3	G98, MC
Modified NDO (MNDO)	G98, MC
Austin Model 1 (AM1)	G98, MC
Parameterized method 3 (PM3)	G98, MC

*C = CADPAC (Amos et al. 1995); GM = GAMESS (Schmidt et al. 1993); G98 = Gaussian 98 (Frisch et al. 1998); J = Jaguar (Jaguar 1998); MO = MOLPRO (Werner and Knowles 1999); MC = MOPAC (Stewart 1993); NW = NWChem (High Performance Computational Chemistry Group 1998)

Equation (24) gives the electronic energy. The electronic wavefunctions $\mathbf{\Phi}$ theoretically have an infinite basis but are in practice approximated by a wavefunction $\mathbf{\Phi}'$ with a finite basis. The size of the wavefunction and its ability to reproduce properties, such as the polarizability and diffuseness of the electron orbitals, have implications on the accuracy of the solutions.

The PES of a system describes the viable chemical processes in the sense that it defines the reaction paths possible (having defined "reaction path" as the minimum energy path). On a PES, one may determine which stationary points are reactants, intermediates, products, and transition states. A stationary point is defined as any point $\mathbf{R}$ where $\partial V_s(\mathbf{R})/\partial \mathrm{R}=\mathbf{0}$. The eigenvalues of the Hessian matrix, $\partial^2 V_s(\mathbf{R})/\partial \mathbf{R}^2$, distinguish between the different kinds of stationary points. Reactants, products and intermediates have all positive eigenvalues, whereas, transition states have exactly one negative eigenvalue. The former describes local minima, and the latter describes first-order saddle points. Figure 3 illustrates these different points in the analytic surface $V_s=\sin(x)\sin(y)$. Points M_1 and M_2 are minima and T is a first-order saddle point. Numerous searching methods have been developed to identify these points in a $3N$-6 dimensional surface, where N is the number of nuclear centers, and these will be discussed in the next section.

Vibrational frequencies may be extracted from the PES by performing a normal mode analysis. This analysis of the normal vibrations of the molecular configurations is a difficult topic and can be pursued efficiently only with the aid of group theory and advanced matrix algebra. In essence, the 3 translational, 3 rotational and $3N$-6 vibrational modes (2 rotational and $3N$-5 vibrational modes for linear molecules) may be determined by a coordinate transformation such that all the vibrations separate and become independent normal modes, each performing oscillatory motion at a well defined vibrational frequency. As a more concrete illustration, assume harmonic vibrations and separable rotations. The PES can thus be approximated by a quadratic form in the coordinates

Figure 3. Hypothetical analytic PES $V_s=\sin(x)\sin(y)$ where V_s is the vertical axis and x and y are the horizontal axes. x and y are in units of (10 × radians). M_1 and M_2 are minima and T is the first order saddle point connecting them.

$$V_s(x_1x_2\ldots) = \tfrac{1}{2}\sum_{i=1}^{3N}\sum_{j=1}^{3N}\frac{\partial^2}{\partial x_i \partial x_j}V_s(x_1x_2\ldots)x_ix_j \tag{25}$$

Where $(x_1x_2\ldots x_{3N})$ = **R**, the configuration matrix. By an appropriate coordinate transformation, an eigenvalue problem arises

$$\mathbf{F}\mathbf{y}_i = \lambda_i\mathbf{y}_i \tag{26}$$

where $\mathbf{y}_i$ are the linearly-independent normal modes; and thus, the elements of the mass-weighted force constant matrix **F** is given by

$$F_{ij} = \frac{1}{\sqrt{m_i m_j}}\frac{\partial^2}{\partial y_i \partial y_j}V_{s'}(y_1y_2\ldots) \tag{27}$$

Note that

$$\mathbf{y}_i = \sum_j c_{ji}\hat{\mathbf{e}}_j \tag{28}$$

where c_{ji} are scalar coefficients and $\hat{\mathbf{e}}_j$ are canonical unit vectors and are the basis of **R**. $V_{s'}$ is in the new basis. The angular frequency corresponding to the ith mode is given by $\omega_i = \lambda_i^{1/2}$, and the vibrational frequency is given by $\nu_i = \omega_i/2\pi$. The eigenvectors determine the amplitude of motion. Therefore, a normal mode analysis determines the vibrational modes, frequencies, and amplitudes of a molecular configuration. (See Kubicki, this volume, for a further discussion.)

To summarize, we have shown that molecular orbital calculations enable the evaluation of parameters needed to compute the rate constant of reactions in the framework of TST. First, quantum mechanics allows the calculation of the PES or, more accurately speaking, portions of the PES that are useful for modeling a reaction. The stationary points of the PES are then identified and these correspond to configurations and energies of reactants, products and transition states. The activation energy can then be evaluated because it is the difference in energy between the transition state and the reactants subject to an energy correction—the ZPE. The complete partition functions can be derived because the configurations are known.

Other rate theories

TST is by no means the only method available to evaluate rate constants, but it is certainly the most widely used. Although TST has been able to make rather accurate predictions regarding reaction rates, it is still an approximate theory, based on classical mechanics and is reliable only for order-of-magnitude estimates of the rate constants. Other rate theories are briefly introduced in this section.

The most complete and detailed computation of the rate allowed by the basic laws of quantum mechanics is given in terms of the S-matrix by (Zhang and Miller 1989; Miller 1975)

$$k(T) = [hQ_r(T)]^{-1}\int_{-\infty}^{\infty} dEe^{-E/kT}N(E) \tag{29}$$

where Q_r is the quantum mechanical reactant partition function per unit volume, N(E) is the cumulative reaction probability

$$N(E) = \sum |S_{n_p n_r}(E,J)|^2 \tag{30}$$

and $S_{n_p n_r}(E,J)$ is the S-matrix, which is the matrix of probability amplitudes for transitions from initial quantum state n_r of the reactant molecules to the final quantum state n_p of the product molecules as a function of total energy E and total angular momentum J. The matrix involves the solution to the Schrödinger equation for each of the transitions and is practically impossible to evaluate.

On the other end of the spectrum is classical rate theory, which is based on classical mechanics. The cumulative reaction probability from this theory is given by

$$N(E) = (h)^{-\mathsf{F}+1} \int d\mathbf{p} \int d\mathbf{q}\, \delta\left[E - \mathbf{H}(\mathbf{p},\mathbf{q})\right] F(\mathbf{p},\mathbf{q}) \chi_r(\mathbf{p},\mathbf{q}) \tag{31}$$

and replaces N(E) in Equation (27). Here, F is the degrees of freedom, **p** and **q** are momentum and coordinates, **H** is the classical Hamiltonian for the complete molecular system,

$$\mathbf{H}(\mathbf{p},\mathbf{q}) = \frac{\mathbf{p}^2}{2m} + V(\mathbf{p},\mathbf{q}) \tag{32}$$

F is the flux

$$F(\mathbf{p},\mathbf{q}) = \frac{d}{dt} \mathrm{h}[f(\mathbf{q})] \tag{33}$$

χ_r is the characteristic function of the reaction

$$\chi_r(\mathbf{p},\mathbf{q}) = \lim_{t\to\infty} \mathrm{h}[f(\mathbf{q}(t))] \tag{34}$$

where h is the Heaviside function, h[x] ={1 for $x > 0$, ½ for 0, 0 for $x < 0$}, f is the dividing surface that separates "reactants" from "products", and $\mathbf{q}(t)$ is the classical trajectory.

In general, all other rate theories fall in between these two end-members. For instance, it was shown by Miller (1998) that TST is an immediate consequence of defining a planar dividing surface for $f(\mathbf{q}(t))$ in Equation (34). Miller (1993) has shown that the separation of variables in TST, i.e., Equation (8), has no quantum mechanical analogues; and therefore, assumptions regarding the coupling between the various degrees of freedom have to be made in formulating a quantum mechanical version of TST. Quantum rate theory is an area of active research (Seideman and Miller 1992, 1993; Manthe and Miller 1993; Thompson and Miller 1995).

A viable alternative for small systems is variational transition state theory or VTST (see Truhlar et al. 1985). Recall that TST makes use of the non-recrossing rule assumption. When recrossing does occur, the assumption results in the over-counting of transitions from reactants to products; that is, the TST rate constant is an upper bound. In VTST, a divide is sought that minimizes these transitions resulting in a minimum rate constant and this divide becomes the basis for the VTST rate constant. We consider, as the simplest example, canonical variational ensemble transition state theory (CVT).

In CVT, just as in TST, the transition state divide (through which the quasi-equilibrium flux is computed) is assumed to be a function only of coordinates and not of momentum. The reference path is taken as the two minimum energy paths from the first order saddle point. The reaction coordinate s is then defined as the signed distance along the reference path with the positive direction chosen arbitrarily chosen. The CVT rate constant is then given by

$$k_r^{CVT} = \min_s \left[k_r^{gen}(T,s) \right] = k_r^{gen}(T, s_c^{CVT}(T)) \tag{35}$$

where k_r^{gen} is a generalized rate constant parametrized by the reaction coordinate s, and s_c^{CVT} is the value of the reaction coordinate at the CVT divide.

Garrett and Truhlar (1979) have shown that the minimum of $k_r^{gen}(T,s)$ corresponds to the maximum of the generalized free energy of activation curve,

$$\Delta G_C^{\ddagger \text{gen}}(T,s) = RT \left[\frac{V_s(s)}{kT} - \ln \frac{Q_C^{\updownarrow gen}(T,s)}{Q_R(T) K^o} \right] \tag{36}$$

(i.e., CVT is equivalent to the maximum free energy of activation criterion). Note that the choice in the divide in CVT involved both "entropic" effects (associated with the partition function ratio) and energetic effects; whereas TST considered only the energy in defining the transition state (hence, the "PES first order saddle point"). In practice, an analytic expression for Equation (36) cannot be written and a curve is fit to calculated points. Truhlar et al. (1985) recommends a five-point curve fit

$$\Delta G_C^{\ddagger \text{gen}}(T,s) \cong c_4(T)s^4 + c_3(T)s^3 + c_2(T)s^2 + c_1(T)s + c_0(T) \tag{37}$$

to Equation (36) where c_i are functions of temperature. Equation (37) is then minimized with respect to s to get s_c^{CVT}. The rate constant is then evaluated using

$$k_r^{CVT} = k_r^{gen}(T, s_c^{CVT}(T)) = \frac{kT\sigma}{h} K^o \exp\left({}^{-\Delta G_C^{\ddagger \text{gen}}(T,s_n)} \big/ _{RT} \right) \tag{38}$$

where σ is the symmetry number of the transition state as in Equation (16), and K^o is the value of the reaction quotient evaluated at the standard state (unity in general). VTST is an actively developing field of research (see Truhlar et al. 1996).

The remainder of this chapter will focus on work using TST. At the current state of development in MO theory, TST is a sufficient framework for elucidating the rate constants of chemical reactions. One should bear in mind that more rigorous and exact theories exist and are actively being developed and these may become more important as increasingly accurate rate constants become needed.

DETERMINATION OF ELEMENTARY STEPS AND REACTION MECHANISMS

Stationary-point searching schemes

In the last section, we demonstrated the potential of determining the rate constant of an elementary reaction by calculating the energies and the partition function of the reactants and the transition state. We discussed that these parameters can be obtained directly through MO calculations if the reactant and transition state configurations are known. How are these configurations determined? In this section, we discuss some of the most common ways to determine these configurations from the PES.

As mentioned previously, reactant and transition state configurations correspond respectively to PES minima and first-order saddle points. Although there is no practical method to find the global minima of any PES, finding the local minima is in general not a difficult problem. Imagine that to get to an energy minimum, one has to start with a configuration reasonably similar to the one sought and "roll down the energy hill" in coordinate space. Any step that reduces the potential energy is a step toward the right direction. This is exactly what the steepest descent calculation (Fletcher and Powell

1963) accomplishes, where the successive step made is the one that initially lowers the energy the most. The steps are taken in the negative direction of the gradient G

$$\Delta \mathbf{x}_k = \mathbf{x}_{k+1} - \mathbf{x}_k = -s\, G_k/|G_k| \tag{39}$$

where $\mathbf{x}_k$ are the mass-weighted position vectors, s is the step size, and the gradient is given by

$$G = \nabla V_s \tag{40}$$

The reason this approach works is that the gradient is always pointing in the up-and-normal direction of the isopotential surface projections on the coordinate space, and each step taken is toward the opposite direction. To give an example in 2D, assume a paraboloid potential energy surface $V_s=x^2+y^2$ (Fig. 4a). Then $G=\nabla V_s=[2x\ 2y]$. Therefore, at the point $(x,y)=(3,4)$, which lies on the isopotential $V_s=V_2=25$, $G=[6\ 8]$. Note that the vector [6 8] is directed up-and-normal to the isopotential surface projection (Fig. 4b). The succeeding step that the steepest descent takes is a coefficient s of a unit vector in the opposite direction.

When the steepest descent calculation begins from a true transition state, it is called the intrinsic reaction coordinate or IRC (Fukui 1981) and the result is a minimum energy path from the saddle point to the minimum. Eckert and Werner (1998) present a quadratic version of steepest descent. Finding energy minima is indeed straightforward except for problematic cases such as searches near flat regions of the PES where the solution could oscillate about a certain value or where intermediates might be missed in the search. In practice, fast second-order or super-linear methods are employed in the determination of minima rather than steepest descent. These methods will be discussed later in the context of finding transition states.

Compared to energy minima searches, finding first-order saddle points is a much more difficult problem. In fact, a great amount of effort in computational chemistry is expended on formulating algorithms to find these elusive configurations and most of

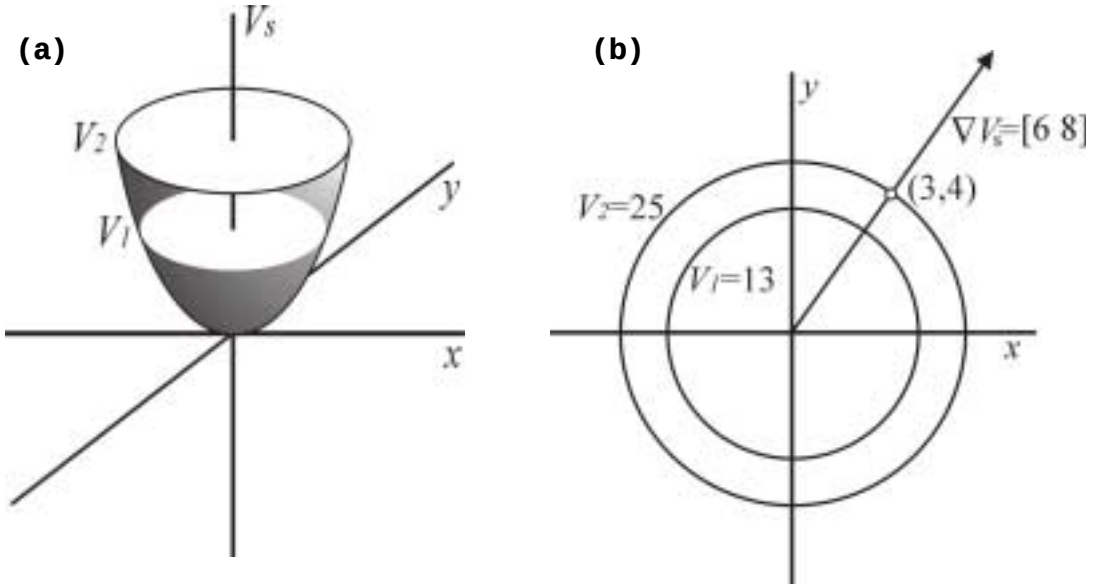

Figure 4. Hypothetical analytic PES $V_s=x^2+y^2$. (a) The surface is a paraboloid with circular isopotentials V_1 and V_2. (b) The gradient $\nabla V=[2x\ 2y]$ always points in the up-and-normal direction of the isopotential projections on the coordinate surface.

MO-TST work goes into finding the transition states. There are in general three stages involved in the search. The first is finding a good initial structure—one that lies within the "quadratic basin" of a saddle point in the PES and is in between two stationary points that are the proposed reactant and product. For reactions involving large numbers of atoms, care must be made that the reactants and the products correspond with each other (i.e., they are indeed connected by a transition state). The second stage is computing a refined transition state from the guessed transition state. Refining a transition state configuration involves efficient algorithms and numerical methods for finding a region of the PES with only one negative eigenvalue. These algorithms can be similar to the methods for determining true energy minima. The last stage is verifying that the transition state connects the reactants and products. This involves the computation and inspection of the IRC from the saddle point to the two adjacent minima.

Transition state initial guesses

Synchronous transit methods. The linear synchronous transit (LST) method put forward by Halgren and Lipscomb (1977) is a simple numerical attempt to find a good transition state guess. In this method, an idealized pathway is first constructed between two structures that are generally reactant and product configurations (i.e., energy minima). The pathway is constructed such that all internuclear distances vary linearly between these path-limiting structures. In particular, the internuclear distances r_{ab} are given by

$$r_{ab}(i) = (1 - f)\, r_{ab,R} + f\, r_{ab,P} \quad a > b = 1 \rightarrow N \tag{41}$$

where f is the interpolation parameter and r_R and r_P are the reactant and the product internuclear distances. These are adjusted by means of a least-squares procedure so as to minimize

$$S = \sum_{a>b}^{N} \frac{\left[r_{ab}(c) - r_{ab}(i) \right]^2}{r_{ab}(i)^4} + 1 \times 10^{-6} \sum_{w=x,y,z} \sum_{a}^{n} \left[w_a(c) - w_a(i) \right]^2 \tag{42}$$

were c and i refer to interpolated quantities. A subsequent constrained optimization is performed on the path maximum using the "path coordinate" p as the fixed parameter

$$p = d_R \Big/ (d_R + d_P) \tag{43}$$

where

$$d_R = \left[\frac{1}{N} \sum_{w=x,y,z} \sum_{a}^{n} \left[w_a(c) - w_a(i) \right]^2 \right]^{1/2} \tag{44}$$

Note that no gradients are used and this method is not computationally as demanding as other methods. However, it often yields a structure with two or more negative eigenvalues and it inherently assumes a simple reaction with one transition state. For these reasons, most computer programs have excluded this option for better search schemes.

The quadratic synchronous method or QST is another method proposed by Halgren and Lipscomb (1977). QST is an improvement of the LST approach in that it searches for a maximum along a parabola connecting reactants and products, instead of a line. That is, in the orthogonal optimization step, the constraint of constant path coordinates is applied by appropriately displacing each resultant structure along a 3-point interpolation, or QST,

pathway likewise defined by the two path-limiting structures. Thus,

$$r_{ab}(i) = \alpha + \beta f + \gamma f^2 \tag{45}$$

And since $r_{ab}(i) = r_{ab,R}$ for $f = 0$ and $r_{ab}(i) = r_{ab,P}$ for $f = 1$, then

$$r_{ab}(i) = (1-f)r_{ab,R} + f r_{ab,P} + \gamma f(1-f) \tag{46}$$

where $\gamma = [r_{ab,M} - (1\text{-}p_m)r_{ab,R} - p_m\ r_{ab,P}]/[p_m(p_m\text{-}1)]$ and M signifies the intermediate structure with path coordinate p_m.

The LST and QST calculations do not actually locate a proper transition state but aim to arrive at structures sufficiently close to it. Ideally, the resulting configuration would lie within the quadratic basin of the first order saddle point and be suitable for input to subsequent transition state searches. However, the synchronous transit methods often yield structures with more than one negative eigenvalue.

Constrained optimization algorithm. The constrained optimization algorithm or "reaction coordinate" or "coordinate driving" approach (Schlegel 1987) is a commonly used procedure that makes use of a fairly simple concept: the reaction path (valley floor) is made up of points, which are in all directions a minimum, except for one—the reaction coordinate. Thus, the reaction path may be constructed by successively incrementing a selected internal coordinate (e.g., bond length or angle) between its path limiting values, while the remaining degrees of freedom are minimized at each step. The constrained internal coordinate, therefore, becomes a proxy for the reaction coordinate and the maximum along this reaction path would be a configuration sufficiently close to the transition state. The method does not necessarily locate a proper saddle point but aids in finding a structure close to it that will be suitable input for a subsequent transition state search. Constrained optimization has a superficial resemblance to the LST method in the sense that it tries to construct a reaction path by changing the configuration using a linearly varying constraint.

Figure 5 demonstrates the use of the constrained optimization approach for the adsorption of water on orthosilicic acid (H_4SiO_4) forming a five-fold coordinate species. Note that the reaction is half of an oxygen-exchange reaction. The best transition state guess is the highest point on the curve.

The choice of the constrained internal coordinate relies heavily on chemical intuition and experience. Consequently, the method has not yet been incorporated in most available quantum chemical programs and perhaps never will be. Despite this, studies have used this procedure with much success. One can construct a software interface to currently existing programs that would effect the constrained optimization algorithm in a semi-automated manner.

Constrained optimization has the advantage of finding intermediates that may have been overlooked, giving a more detailed picture of the topology of the PES. Furthermore, constrained optimizations often provide better starting guesses for transition state searches. Failure to find a transition state in the forward direction may be solved by locating it in the reverse direction. This also serves as an internal check to see if the reactants and products do correspond to each other and may lead to the discovery of new minima.

Because many increments may be required to complete the reaction path, this approach can become expensive particularly for large molecules. Another disadvantage is that different choices of "reaction coordinate" can produce different reaction pathways, which is not of particular concern in classical transition state theory because we are only

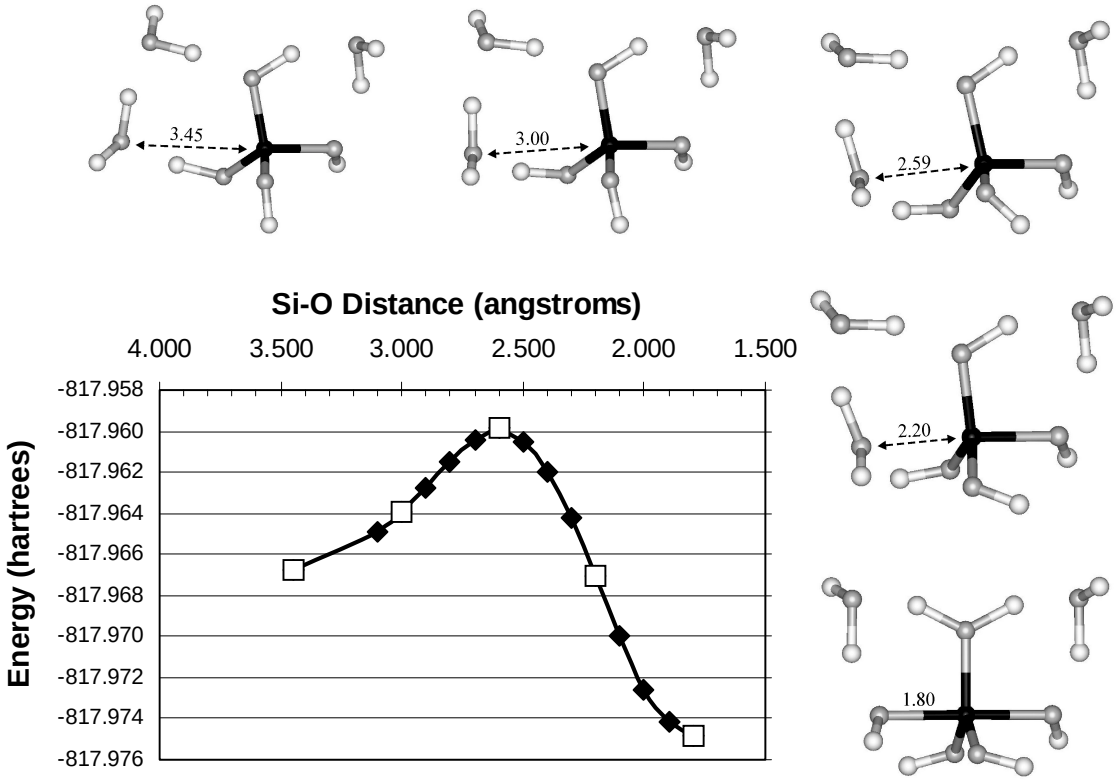

Figure 5. The constrained optimization approach applied to the adsorption of water onto orthosilicic acid, $H_2O + H_4SiO_4 \rightarrow H_2O{\cdot}H_4SiO_4$. The inset is the potential energy-constrained parameter diagram (where the potential energies are *ab initio*; calculated at the B3LYP/3-21G(d) level). Light-gray spheres are hydrogen, medium-gray spheres are oxygen and black spheres are silicon. The configurations are plotted in the diagram as open squares, and other intervening points are in solid diamonds. The step size used in the procedure is 0.1 Å. The middle configuration has been optimized to a transition state.

interested in the minima and saddle point configurations. The pathways may be discontinuous, may fail to contain the transition state, and may even fail to yield stable limiting structures. These may sometimes be corrected using a change in choice of the constrained coordinate. The problems associated with the method are described by Halgren and Lipscomb (1977).

Dewar-Healy-Stewart method. A method similar to the constrained optimization approach was proposed by Dewar et al. (1984). In their method, the reactant and product coordinates are superimposed to maximum coincidence and a "reaction coordinate" is defined. The lower-energy endpoint is then modified using the chosen "reaction coordinate" and is incremented closer to the higher energy endpoint. The energy is then optimized subject to the condition that the "reaction coordinate" remains fixed. This procedure is done iteratively until the two geometries are sufficiently close to each other to define a good transition state guess.

Intuition, experience, and the Hammond postulate. Subjectivity plays a huge role in most transition state searches. For example, the choices for the reactant and product configurations can be arbitrary (there are frequently several minima to choose from), guided possibly by experience from laboratory experiments or previous calculations on similar systems. One may also choose a pair on the basis of having the least amount of undue change from one another; for example, molecule subgroups that are not

participating directly within the reaction remain essentially the same. Subjectivity is enhanced when dealing with larger systems. For instance, while the lowest energy configurations possible are the ideal choices for path limiting configurations, there is actually no guarantee of finding the global minimum of any PES unless the entire PES is mapped. Hence, the initial configurations chosen for reactant and products can influence the calculated reaction pathway.

Frequently, the above-mentioned numerical procedures would all fail to yield a satisfactory transition state guess, or worse lead to one that is irrelevant to the mechanism of concern. There are occasions when the problem is an incompatible reactant-product pair. At other times, the numerical methods cannot make good guesses despite the reactant-product pair being good choices. A few guidelines in making good guesses are in order.

A guide to follow is that good transition state guesses lie, with some modifications, somewhere between the reactant and product (or intermediate) structures. Transition states therefore share some properties of both. This is in fact the basis for most of the numerical methods for finding good guesses. Another guide is the Hammond postulate, which can be useful in locating the transition state in the exothermic direction. The postulate roughly states that if there is almost no activation energy for a strongly exothermic reaction, the starting materials and transition states will be nearly identical in configuration (Leffler 1953; Hammond 1955). The concept is schematically illustrated in Figure 6 where the transition state $XYZ^{\ddagger}$ is perceived to have traveled a lesser distance in coordinate space when in a highly exothermic reaction having a low activation-energy.

A suspected transition state guess may be made better by fixing several parameters related to the reaction and optimizing the rest of the degrees of freedom. The constrained parameters can then be released one at a time until only one or two are left. The result of this kind of optimization can be a reasonable transition state guess.

Optimization to stationary points

Newton's method. A good place to begin the discussion on finding stationary points, particularly transition states, is Newton's method because it is the foundation for most of the other methods as well. The analyses of the PES (see Head and Zerner 1989) begins in the Taylor expansion about a given point **a**

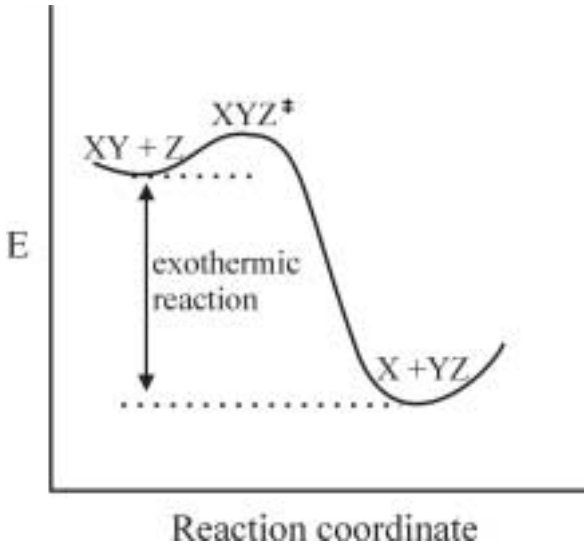

Figure 6. Highly exothermic reaction with low activation energy barrier. The Hammond postulate predicts that $XYZ^{\ddagger}$ would be similar to XY+Z.

$$V_s(\mathbf{x}) = V_s(\mathbf{a}) + G^{\mathsf{T}}\Delta\mathbf{x} + \tfrac{1}{2}\Delta\mathbf{x}^{\mathsf{T}}H\Delta\mathbf{x} + \ldots \tag{47}$$

where $\mathbf{x} = \mathbf{a} + \Delta\mathbf{x}$ and the Hessian is given by

$$H = \nabla\nabla^{\mathsf{T}}V_s \tag{48}$$

Typically, the expansion is truncated at the quadratic term. The stationary condition is invoked

$$\frac{\partial V_s}{\partial \Delta x} = 0 \tag{49}$$

giving a linear set of equations

$$H\Delta\mathbf{x} = -G \tag{50}$$

and thus a unique solution

$$\Delta\mathbf{x} = -H^{-1}G \tag{51}$$

provided H is non-singular. Hence, each successive step is defined by the inverse of the Hessian and the gradient. Note that this works equally well for minima and saddle points provided the search has the right curvature and there is an accurate way to update the gradient and the Hessian for each step. Hessian update formulas include Broyden-Fletcher-Goldfarb-Shanno (BFGS) and the Davidson, Fletcher, and Powell (DFP) equations (see Press et al. 1992).

The Hessian is symmetric and may therefore be diagonalized to yield a set of real eigenvalues b_i associated with orthonormal eigenvectors v_i. Equation (51) can therefore be represented as

$$\Delta x = -\sum_i v_i^{\mathsf{T}} G v_i / b_i \tag{52}$$

Here v_iG is the component of G along v_i. Observe that the step is directed opposite to the gradient along each mode with a positive H eigenvalue and along the gradient of each mode with a negative H eigenvalue. Hence, if the Hessian has the correct curvature, the step would do exactly as desired for a transition state search going up the direction of the negative mode while going down in the other positive modes. Likewise, for minima searches, it will go down the positive modes. In general, this procedure would look for the nearest stationary point.

The convergence of the Newton-Raphson is quadratic and fast. Proofs for the quadratic convergence of the method are given by Fletcher (1987) and Dennis and Schnabel (1983).

Eigenvector following. The eigenvector following (EF) method proposed by Cerjan and Miller (1981) develops from the Newton-Raphson procedure. The main problem with the Newton-Raphson procedure is that if the Hessian is in a region that has the wrong curvature (non-quadratic), there is no guarantee that the stepping procedure would correct itself, and the computation may wander about aimlessly in the PES until it fortuitously finds a better region.

Cerjan and Miller (1981) showed that there exists a step that is capable of guiding the calculation away from the current position and to search for another stationary point. The modification to Equation (52) is minor

$$\Delta x = -\sum_i v_i^{\mathsf{T}} G v_i /(b_i - \lambda) \tag{53}$$

but the implications are significant and has led others to proceed from the same analysis (e.g., Banerjee et al. 1985). The problem of finding the next best step is then replaced by finding the correct scalar λ. Cerjan and Miller (1981) suggest the iterative solution of

$$l^2 = G(\lambda I - H)G(\lambda I - H) \tag{54}$$

where l is a predetermined step size. Their algorithm is a type of trust-region minimization method; that is, in each step, it attempts to determine the lowest energy within a hypersphere of radius l and takes the step to that point.

Rational functional optimization. The rational functional optimization or RFO (Banerjee et al. 1985; Baker 1986, 1987) is another method that develops from the Newton-Raphson procedure. Essentially, Equation (47) is rearranged and modified into a "rational functional"

$$\in = V_s(x) - V_s(a) = \frac{G^{\mathsf{T}}\Delta x + 1/2\Delta x^{\mathsf{T}} H \Delta x}{1 + \Delta x^{\mathsf{T}} S \Delta x} = \frac{1/2\begin{pmatrix}\Delta x^{\mathsf{T}} & 1\end{pmatrix}\begin{pmatrix} H & G \\ G^{\mathsf{T}} & 0\end{pmatrix}\begin{pmatrix}\Delta x \\ 1\end{pmatrix}}{\begin{pmatrix}\Delta x^{\mathsf{T}} & 1\end{pmatrix}\begin{pmatrix} S & 0 \\ 0 & 1\end{pmatrix}\begin{pmatrix}\Delta x \\ 1\end{pmatrix}} \tag{55}$$

where S is a symmetric scaling matrix often taken as the unit matrix. If we differentiate Equation (55) and invoke the stationary condition as in Equation (49), we get the eigenvalue equation

$$\begin{pmatrix} H & G \\ G^{\mathsf{T}} & 0\end{pmatrix}\begin{pmatrix}\Delta x \\ 1\end{pmatrix} = \lambda\begin{pmatrix} S & 0 \\ 0 & 1\end{pmatrix}\begin{pmatrix}\Delta x \\ 1\end{pmatrix} \tag{56}$$

where $\lambda = 2\in$. This can be separated out into two linear relations. Taking S as the unit matrix, we get

$$(H - \lambda I)\Delta \mathbf{x} = \mathbf{0} \tag{57}$$

$$G\Delta x = \lambda \tag{58}$$

If we express Equation (57) in terms of a diagonal Hessian representation, it rearranges to Equation (53). Substituting Equation (58), we get

$$\lambda = -\sum_i v_i^{\mathsf{T}} G v_i^{\mathsf{T}} G v_i /(\lambda - b_i) \tag{59}$$

which can be solved iteratively to find λ. This is the shift parameter prescribed by Banerjee et al. and it is considered better (Frisch et al. 1998) than that proposed earlier version of Cerjan and Miller.

Combined methods. There are numerous other methods in the literature for finding transition states. However, the more common methods use simpler numerical algorithms in a more efficient way. The Berny optimization algorithm and the synchronous transit quasi-newton method (STQN) are good examples.

The Berny algorithm (Frisch et al. 1998) is not a single algorithm but one that has evolved through use. It is based on the method developed by Schlegel (1982), which was a conjugate gradient method (see Press et al. 1992) modified to update the Hessian in a specific way. The current method is a RFO procedure using a quadratic step size for a

transition state search (or a linear step size for a minimization step). The original Hessian update method has been kept but modified to handle redundant internal coordinates; optimizations in general are considered best performed in redundant internal coordinates following the work of several workers (Peng et al. 1996; Pulay et al. 1979; Pulay and Fogarasi 1992; Fogarasi et al. 1992). The Berny algorithm still needs a starting guess fairly close to the transition state to arrive at a proper transition state in a reasonable amount of time.

The STQN method, devised by Peng and Schlegel (1994), combines the LST or QST approach for the initial guess and the EF method to optimize to a transition state. The EF steps are guided by the tangent to the arc of circle passing through the initial transition state guess and the corresponding minima. The STQN internally provides a transition state guess, although the guess is only as good as what the LST or QST methods supply.

Other procedures combine transition state searches with reaction path following. For example, Ayala and Schlegel (1997) designed a procedure that uses the STQN method and a reaction path searching method described by Czerminski and Elber (1990) to find the entire reaction path. The primary advantage of these procedures is the convenience of automation. For TST purposes however, the entire reaction path is not necessary; it is sufficient to determine two minima and the transition state that joins them.

MO-TST STUDIES IN THE GEOSCIENCES

Introduction and definitions

Spurred by the rapid increase in the power of computers, MO theory and numerical implementation have recently become fast evolving fields. As a consequence, the developments in MO theory and implementation have given new life to the mature field of TST as can be evidenced in the rising number of MO-TST studies in the different branches of material and life sciences. As a result, TST is being challenged, opening opportunities for improvement of TST and the development of new rate theories.

There are two natural subdivisions of MO-TST studies based on the kind of reactions being studied. Studies that aim to simulate a system that has only one phase we shall refer to as homogeneous reaction MO-TST; whereas those that aim to simulate a system with two or more phases we shall refer to as heterogeneous reaction MO-TST. Although this distinction is convenient, we should keep in mind that most overall reactions of geological significance are ultimately a mixture of both kinds of elementary reactions.

Systems in MO-TST studies may be approached using two different treatments of boundary conditions. In “conventional” or “finite MO”, a structure containing a “cluster” of atoms is chosen to represent the bulk (Lasaga 1992). Therefore, it is assumed that all the significant interactions are considered when localized calculations are made on the site of interest, possibly with one or several shells of neighboring atoms or molecules. Hence, conventional MO is ideally suited for gas-phase reactions, reasonably suited for liquid phases, and questionably suited for solid phases. For most rock-forming minerals, conventional MO studies would usually involve breaking of covalent bonds between atoms and terminating them with an atom or group of choice. The proper ways to terminate these “edges” has been a major topic of discussion covered by various studies (e.g., Nortier et al. 1997; Fleisher et al. 1992; Hirva and Pakkanen 1992; Lindblad and Pakkanen 1993; Manassidis et al. 1993; Hagfeldt et al. 1992). The task is left for the modeler to choose the appropriate clusters, deciding how to terminate and justifying the choice for termination through comparisons with experimental data such as geometry, binding energies and electron density and Laplacian maps (see Gibbs, this volume, for a

discussion on Laplacian maps). The majority of MO-TST work done on minerals utilizes conventional MO and this is mostly due to the early development of the underlying theory and numerical algorithms to conduct stationary point searching. Gaussian (Frisch et al. 1998), GAMESS (Schmidt et al. 1993), CADPAC (Amos et al. 1995) and Jaguar (Jaguar 1998) are good examples of conventional MO program packages.

A recently applied and conceptually appropriate method for minerals is to find a periodic wavefunction solution to the repetitive unit cell structures (Pisani and Dovesi 1980; Saunders 1984; Pisani et al. 1988). In these methods, the boundaries are treated as periodic and the unit cell structures infinitely repeating, and we shall refer to this as "periodic MO." An example of the implementation of this is the CRYSTAL (Orlando et al. 1999; Pisani et al. 2000) program. Recently, geometry optimization code for the determination of minima and saddle points has been provided with the standard issue of CRYSTAL 98. It is yet to be demonstrated how transition state calculations from these methods compare with data gathered from conventional MO methods and how they agree with actual experiments. While optimizations to minima using periodic MO have become routine procedures (e.g., Civalleri et al. 1999; Gibbs et al. 1999; Rosso et al. 1999), there has been a dearth of calculations using this method on transition states. Certainly, periodic MO implementations are computationally more demanding than conventional MO methods and less number of studies have been conducted using these. Recently, Sierka and Sauer (2000) have successfully performed periodic MO-TST using CRYSTAL 98. It should be noted that in CRYSTAL 98, there are no analytical gradients and the numerical procedure is tedious. NWChem (High Performance Computational Chemistry Group 1998) offers geometry optimization to minima and transition states for both conventional and periodic MO. We know of no published periodic MO-TST studies using NWChem to date.

Numerous MO-TST studies that are relevant to the geosciences have been conducted, and we review them in this section. Mineral-water interactions have been the focus of several studies particularly those related to the weathering of rocks. These predominantly involve dissolution and precipitation reactions of common rock-forming minerals and are mostly heterogeneous reaction MO-TST. A number of atmospheric reactions have been the focus of attention because of their relevance to environment and climate change. Phenomena such as the ozone hole, pollution, the greenhouse effect, and more local applications such as acid rain are a number of problems MO-TST aids in explaining. Finally, there are a few other areas where MO-TST is being used such as petroleum systems and surface catalysis.

Reaction pathways of mineral-water interaction

Quartz. Due to the simple chemical composition of quartz and its sheer ubiquity in crustal rocks, its reaction with water is perhaps one of the most extensively studied mineral dissolution processes using MO-TST methods. We are gaining a better understanding of the molecular level mechanisms on two main fronts: quartz dissolution, and isotope exchange reactions of quartz with water. Understanding the nature and quantifying the rates of the dissolution reactions of quartz is important in understanding the rates of weathering of landforms and continents on the grand scale, and of the leaching of minerals on the microscopic scale. Elucidating isotope exchange of quartz with water is important in determining fluid sources, flow rates, and volume.

The pioneering work of Lasaga and Gibbs (1990) paved the way for using the MO-TST approach in systems of rock-forming minerals. Aside from supplying a review for the basic theory for *ab initio* methods and transition state theory, the study aimed to analyze the silicate-water reactions using conventional MO-TST. The elementary

reaction modeled was

$$H_3SiOH + H_2O^* \rightarrow H_3SiO^*H + H_2O \quad (60)$$

up to the MP2/3-21G(d) level. (We will henceforth use the method/basis-set nomenclature of Hehre et al. 1986). The actual reaction modeled was therefore the gas-phase hydroxyl-group exchange reaction of a silanol molecule with a water molecule. Figure 7 shows the complete animated reaction "movie." This, they argue, has bearing on the silica dissolution itself, where the abstracted hydroxide group can be thought of as representing silanolate ($-OSiH_3$) and the hydrogens attached to the silicon representing the rest of the quartz crystal. Remarkably, their best calculation of this "dissolution" process has an activation energy that is indeed close to the experimental activation energy of dissolution (64 kJ/mole calculated versus 75 kJ/mole experimental). They predicted kinetic isotope effects, KIE=$k_{f,D_2O}/k_{f,H_2O}$ at different temperatures. For example, they determined that the rate constant of the D_2O reaction is slower by a factor of 0.307 than the H_2O at 298K. As will be seen later on the paper by Casey et al. (1990), this is off by more than a factor of two compared to experimental results. The mechanism that Lasaga and Gibbs (1990) determined is suited for a study on oxygen isotope exchange as well, but parameters for this reaction were not calculated.

The transition state was successfully located by a successive combination of the LST method, the constrained optimization approach, and a final full optimization using the Berny algorithm. From the transition state, the steps toward the reactants were generated

Figure 7. Configurations along the reaction coordinate of $H_3SiO^*H + H_2O \rightarrow H_3SiOH + H_2O^*$. [Used by permission of American Journal of Science, from Lasaga and Gibbs (1990), *American Journal of Science,* Vol. 290, Fig. 20, p. 290].

by "nudging" (incrementing) along the direction of the eigenvector that corresponds to the negative eigenmode and subsequently performing a steepest descent calculation. This procedure is equivalent to an IRC calculation.

The Lasaga and Gibbs (1990) study established several key points regarding silica dissolution that are now generally accepted. First, there is an energetically plausible exchange reaction where the silicon atom of silica becomes an electron acceptor and the oxygen of water becomes a donor. Second, this dissolution reaction has a five-fold coordinate intermediate that is a recurring configuration for the reactions of silica (Kubicki et al. 1993; Badro et al. 1997; and references within). Third, the corresponding transition state configuration depicts the hopping of a hydrogen atom. Lastly, the energetically preferred mode of adsorption of water is by donor adsorption wherein the proton of a terminal hydroxide hydrogen bonds to the oxygen of water and is not the mode of adsorption that causes the reaction to occur.

A companion paper to Lasaga and Gibbs (1990) is the experimental and *ab initio* work of Casey et al. (1990). The study was conducted to examine the causes of the kinetic isotope effect in silica dissolution by combining careful experimentation using D_2O and H_2O as solvents, and results from *ab initio* calculations. The reaction investigated was

$$H_6Si_2O + H_2O \rightarrow 2H_3SiOH \tag{61}$$

and the reaction modeled was therefore the gas phase hydrolysis of disiloxane, H_6Si_2O. The study was conducted up to the MP2/6-31G(d) level, which is a more accurate calculation than the previous calculation of Lasaga and Gibbs (1990). Note that in this conventional MO-TST treatment, a hydride (H^-) terminated cluster is being used to represent quartz just as in the previous work. The transition state was determined by constrained optimizations followed by a Berny optimization.

Aside from the larger molecular size for the representative reaction, the kinetic isotope effects at different temperatures were evaluated using more sophistication than the previous study. Quantum tunneling corrections were incorporated in the calculations. In general, the experimental and *ab initio* results did not agree to a significant degree. Because the mechanism found in the *ab initio* treatment involved the transfer of hydrogen and had a significantly depressed $k_{f,D_2O}/k_{f,H_2O}$ compared to the experiment, the conclusion was that hydrogen transfer occurred either before or after formation of the transition state complex during the reaction.

Several useful points can be made from this study. First, the reaction with the larger cluster agrees with results from the previous smaller cluster reaction of Lasaga and Gibbs (1990), in that the silicon is an electrophilic site and can bond with the oxygen of water forming five-fold coordinate silicon. Second, the quantitative predictive capabilities of *ab initio* calculations need to make use of larger clusters, and possibly a consideration of the hydration spheres. Third, the rate-determining step appears to involve the Si-O bond lengthening process. Lastly, a precursor elementary reaction to the dissolution process may involve a rapid hydrogen transfer to the bridging oxygen atoms.

As previously pointed out by Lasaga and Gibbs (1990), there is reason to believe that the hydroxide exchange reaction between water and quartz proceeds by way of a five-fold coordinate silicon intermediate. The existence and nature of this five-fold coordinate silicon atom was further investigated by Kubicki et al. (1993). They determined the gas-phase reaction path of the addition of hydroxide to orthosilicic acid and a subsequent abstraction of H_2O.

$$H_4SiO_4 + OH^- \rightarrow H_5SiO_5^- \rightarrow H_3SiO_4^- + H_2O \tag{62}$$

The computation was performed up to the MP2/6-31G(d) level. They gathered evidence suggesting that the five-fold coordinate silicon structure may be a long-lived intermediate in basic solutions and can possibly be observed experimentally (Kinrade et al. 1999). The technique they used in finding the transition state was primarily constrained optimizations followed by Berny optimization.

More elaborate and ambitious studies on the dissolution reactions of silica were conducted by Xiao and Lasaga (1994, 1996). Their objective was to provide full descriptions of the reaction pathway of quartz dissolution in acidic and basic solutions, from the adsorption of H^+, H_2O or OH^- on a site, the formation of possible reaction intermediates and transition states, to the hydrolysis of the Si-O-Si bonds. Also, their aim was to extract kinetic properties such as changes in activation energy, kinetic isotope effects, catalytic and temperature effects, and the overall rate law form. The reaction mechanisms investigated were

$$H_6Si_2O + H_2O \rightarrow H_6Si_2O\text{-}H_2O \rightarrow 2H_3SiOH \tag{63}$$

$$H_6Si_2O + H^+ + H_2O \rightarrow H_3SiOH + H_3SiOH_2^+$$

$$H_6Si_2O_7 + OH^- + H_2O \rightarrow H_4SiO_4 + H_3SiO_4^-$$

Note that the first two reactions relate to disiloxane and the last one relates to orthosilicic acid. These reaction paths were analyzed up to the MP2/6-31G(d) level, and the transition states were determined by constrained optimizations and Berny optimization. The main conclusions of this work were clearly outlined by Lasaga (1995). These studies demonstrated that the neutral and acidic reaction mechanisms both have a single energy barrier and the basic reaction mechanism has two energy barriers. Furthermore, the calculations showed how catalysis occurs when hydronium or hydroxide is in the dissolution reaction.

Kinetic isotope effects were reported for both of these studies and showed significant departure from experimental results both in magnitude and direction. This shows that either the experimental data are inaccurate, the mechanism determined is erroneous (possibly due to the inability of the model to simulate the complex system), or the true KIE is a result of a weighted average of isotope effects from several elementary steps controlling the rate.

Several comments deserve mention regarding the previous dissolution studies Lasaga and Gibbs (1990), and Xiao and Lasaga (1994, 1996). A possible reason for the discrepancies between *ab initio* results and experiments with respect to the activation energies is the omission of hydration spheres in the surface of quartz. As suggested by Lasaga (1995), nearest neighbor water molecules may play a major role in defining the energetics of quartz-water reactions. Lasaga (1995) has shown that the adsorption energies of several optimized configurations indeed show that there is preference for three or more adsorbed water molecules on the surface of quartz. Another probable reason is the contribution of the enthalpy of proton exchange reactions to the value of the experimentally measured activation energy (Casey and Sposito 1992).

A related study is that of Felipe et al. (2001). While previous work on silica has emphasized mainly an understanding of the dissolution process, this recent study has shifted focus to the mechanisms and rates of isotope exchange reactions. The aim of this recent study was to quantitatively determine the rate at which hydrogen isotope exchange occur, while considering the first sphere of hydration as well as long-range interactions using a dielectric continuum model. The reactions investigated were

$$Si(OH)_4 + HOH^* + 2H_2O \rightarrow Si(OH)_3OH^* + 3H_2O \tag{64}$$

$$Si(OH)_4 + HOH^* + 6H_2O \rightarrow Si(OH)_3OH^* + 7H_2O$$

The reactions were analyzed up to the B3LYP/6-31+G(d,p) level and the transition states were determined using constrained optimization and Berny optimization. The reactants and transition states determined are shown in Figure 8. The energetically favored reaction path found is a Grötthus type of reaction (Bernal and Fowler 1933) where a hydrogen atom transfers to the nearest water molecule whose hydrogen likewise transfers to the next nearest water molecule and so on effecting hydrogen transfer.

An absolute rate of isotope exchange curve is obtained (10^6 s^{-1} at 298 K) although no comparison can be made because the experimental values have not yet been determined. The zero-point corrected activation energy for the exchange is 31 kJ/mole, which is not unreasonable. Experimental values for isotope equilibrium for this exchange at 350°C by Kuroda et al. (1982) and Ihinger (1991) are in good agreement with those derived from MO values ($R_{min}/R_{water} = \alpha_{\sim OH\text{-}H_2O} = 0.968$ from experiment versus $\alpha_{\sim OH\text{-}H_2O} = 0.971$

Figure 8. Configurations along the reaction coordinate of $Si(OH)_4 + HOH^* + 2H_2O \rightarrow Si(OH)_3OH^* + 3H_2O$. The two minima and transition states are optimized. White spheres are hydrogen, gray spheres are oxygen and black spheres are silicon.

calculated) suggesting that the mechanism is a plausible contributing reaction to the equilibria. A tabulation of some of the best activation energy data of silica-water reactions derived from MO-TST is shown in Table 2.

There are several areas where the MO-TST studies of quartz aqueous reactions can be improved. The studies that have been conducted made use of relatively small systems employing mainly conventional MO-TST. Therefore an improvement would be to design simulations that can distinguish between the different bridging oxygen atoms of quartz. Larger clusters may be employed (e.g., Kubicki et al. 1996; Pereira et al. 1999; Pelmenschikov et al. 2000) as well as the consideration of the aqueous media either through dielectric continuum methods or adding additional water molecules. Note however that the use of larger clusters increases the problem of intramolecular hydrogen bonding, which alters the simulated stability of surface complexes and speciation of the surface. Alternatively, the use of either periodic structures (e.g., Civalleri et al. 1999), or embedding of clusters in a charge field (Pisani and Ricca 1980) may be appropriate.

Feldspar. Another ubiquitous material in crustal materials is feldspar making the study of its dissolution reaction highly relevant to understanding the weathering of continents. Concurrent with the study of quartz dissolution, Xiao and Lasaga (1996) investigated the mechanism of feldspar dissolution in acidic pH conditions. The gas phase reaction paths

$$H_6SiOAl + H_2O \rightarrow H_6SiOAl\text{-}H_2O \rightarrow H_3SiOH + H_3AlOH \qquad (65)$$

$$H_6SiOAl + H^+ + H_2O \rightarrow H_3SiOH + H_3AlOH_2^+$$

in addition to Equation (63), were investigated in order to simulate the bonds present in albite. These were simulated up to the MP2/6-31G(d) level. The transition states were obtained using constrained optimizations and Berny optimization. The main result of the study is that the hydrolysis of Si-O-Al follow somewhat the same pathway as the hydrolysis of Si-O-Si. The Si-O-Al bonds are demonstrated to hydrolyze faster than the

Table 2. Silica-water reaction zero-point corrected activation energies for the forward direction. Note the marked dependence on the size of the system and the method/basis-set.

Reaction	E_a (kJ/mole)	MO Level	Ref.
Hydrolysis:			
$H_6Si_2O + H_2O = 2H_3SiOH$	133.8	MP2/6-31G(d)	[1]
$H_6Si_2O_7 + H_2O = 2H_4SiO_4$	119.3	MP2/6-31G(d)	[1]
$H_5Si_2O_7^- + H_2O = H_7Si_2O_8^-$	90.37	HF/6-31G(d)	[2]
$H_7Si_2O_8^- = H_4SiO_4 + H_3SiO_4^-$	23.8	HF/6-31G(d)	[2]
$H_6Si_2O + H_3O^+ = H_3SiOH + H_3SiOH_2^+$	94.06	MP2/6-31G(d)	[3]
Exchange:			
$H_3SiO^*H' + H_2O = H_3SiOH + HO^*H'$	127.3	MP2/6-31G(d)	[1]
$(OH)_3SiO^*H' + H_2O = (OH)_3SiOH + HO^*H'$	117.9	MP2/6-31G(d)	[1]
$(OH)_3SiOH + H'OH + 2H_2O = (OH)_3SiOH' + HOH + 2H_2O$	52.51	B3LYP/6-31+G(d,p)	[4]
$(OH)_3SiOH + H'OH + 6H_2O = (OH)_3SiOH' + HOH + 6H_2O$	31.5	B3LYP/6-31+G(d,p)	[4]

References: [1] Lasaga 1995; [2] Xiao and Lasaga 1996; [3] Xiao and Lasaga 1994; [4] Felipe et al. 2001

Si-O-Si. Again, the major results of this study were clearly outlined by Lasaga (1995) and will not be discussed here.

Zeolites. Because of their importance in industrial catalysis, there has been a sustained interest on reactions involving zeolites. Numerous MO-TST studies have therefore been done although most of these involve systems relevant to the petrochemical industry rather than natural phenomena. Nevertheless, these have given new insight in understanding surface phenomena and dealing with large systems. Recent work by Sierka and Sauer (2000) involving mechanisms of hydronium ion hopping from one surface SiOAl site to another compared calculations of conventional MO-TST, periodic MO-TST, and a combined quantum-mechanical and potential-function method that they developed. They determined that the combined approach, which was computationally less expensive than the two other methods, yielded comparatively similar results. Fermann et al. (2000) also investigated the same mechanisms using conventional MO-TST and comparing different high-level *ab initio* methods.

Halite. Recent interest on the dissolution reaction of halite is due to the significance of NaCl in atmospheric chemistry. Oum et al. (1998) has recently shown that airborne hydrated sea-salt microparticles are involved in the photolytic formation of chlorine by reaction with ozone. Little is actually known about the mechanisms of the dissolution process of the familiar table salt. In general, it is assumed from casual observation that the dissolution occurs stoichiometrically, with a decrease in free energy, and with a low activation energy.

In a recent paper, Jungwirth (2000) sought the least number of water molecules to hydrate sodium chloride by computing the reaction coordinate from a crystalline state to a hydrated state. This study used a conventional MO approach to examine the reaction

$$NaCl + 6H_2O \rightarrow Na^+ + Cl^- + 6H_2O \qquad (66)$$

up to the MP2/6-311G(2d, p) level. The exact method to determine the transition state was not mentioned although it is highly likely that either STQN or Berny method was used.

Atmospheric reactions of global significance

The chemistry of the atmosphere is complicated and convoluted because myriad species are interacting in thermal and photochemical reactions. Numerous MO-TST studies have been conducted to help understand various aspects of the reactions of atmospheric chemistry. It will not be possible to cover every reaction studied in atmospheric chemistry in this review, but we focus on recent work related to some of these.

Ozone and nitrogen compounds. An extremely important characteristic of the present atmosphere is the presence of ozone. This gas is primarily formed from the interaction of photons ($\lambda < 240$ nm) with oxygen gas. The basic reactions of ozone chemistry were discussed by Chapman (1930) and are still valid. Ozone in the stratosphere is beneficial to life, absorbing ultraviolet light and shielding the surface of the earth from the harmful rays. On the other hand, ozone in the troposphere is undesirable and even harmful, being a component of smog in urbanized areas. These properties make the study of ozone and ozone-related reactions important and exciting. The potential energy surface for the ozone molecule have been worked out in great detail both analytically (e.g., Atabek et al. 1985, Murrell and Farantos 1977) and numerically (e.g., Rubio et al. 1997; Xantheas, et al. 1991).

The primary reason for the attention gained by ozone related reactions is the

discovery that the protective ozone shield in the stratosphere has a growing "hole" over Antarctica (Farman et al. 1985). Several species have been found to react with and consume the gas. In general, the reactions for the primary "consumers" of ozone is given by

$$X + O_3 \rightarrow XO + O_2 \quad (67)$$

where X=(•NO, •Cl, •OH) – the dots indicate that X is a free radical species. (Note that the reverse processes are also possible, and XO may be thought of as a generalized ozone "producer"). The rates of Equations (67) have been well-constrained using experimentally derived rate constants and are tabulated along with other atmospheric data by DeMore et al. (1992). However, the sources of these ozone consumers (and producers) are less understood and have been the focus of recent intense study. It is now known that a substantial number of pathways are possible and need to be considered in elucidating the composition and chemical behavior of the atmosphere. Furthermore, these consumers may be (1) reproduced after reacting with ozone effecting a catalytic pathway, (2) react with other species that produce more ozone than they themselves consume, or (3) be involved in some other pathway yet unexplored. In other words, the relationship between these species and ozone is not simple. The problem that MO-TST helps to solve, therefore, is the determination of the pathways and the rate constants of these reactions.

For the ozone hole problem, nitrogen compounds play a key but indirect role. (Arguably, the most extensively involved substances in the balance of ozone in the stratosphere and troposphere are the compounds of nitrogen by virtue of abundance and reactivity). It is now generally accepted that the depletion of ozone in the Antarctic stratosphere is primarily due to the direct action of chlorine free radicals with ozone. The existence of these free radicals is facilitated by two nitrogen compounds, nitric acid trihydrate (NAT, $HONO_2 \cdot 3H_2O$) and one of the atmospheric chlorine reservoirs, $ClONO_2$ (Brune et al. 1991; Schoeberl and Hartmann 1991). During the southern-hemisphere winter, NAT precipitates in the extremely cold Antarctic winter stratosphere. These crystals then become sites where hydrochloric acid (HCl), the other main chlorine reservoir, condenses. Subsequently, gaseous $ClONO_2$ then reacts with HCl in NAT forming chlorine gas

$$ClONO_2(g) + HCl_{\text{diss in NAT}} \rightarrow HONO_2 + Cl_2 \quad (68)$$

The chlorine gas is then free to dissociate into chlorine free radicals mediated by photons. Equation (68) is heterogeneous and has been investigated using MO-TST methods by Bianco and Hynes (1999), Xu and Zhao (1999) and Mebel and Morokuma (1996). Details of the reaction such as the activation energies, the ionization of HCl, the catalysis in the presence of water molecules, and the action of other catalysts such as nitrate (NO_3^-) have been investigated.

Other nitrogen compounds are actively being investigated to determine the implications of their release in the atmosphere. For example, nitrous oxide has lately been the focus of several studies due to its formation in the combustion of solid rocket propellants. Through the combustion process, HONO is directly introduced into the troposphere and stratosphere. The decomposition of organic nitrates in fertilizers also contributes to HONO in the troposphere. Nitrous oxide has the potential of dissociating into two different reactive species •OH and •NO (Baulch et al. 1982) although this is not the only reaction it may undergo, and other reactions are actively being investigated.

For example, Mebel et al. (1998) conducted MO-TST studies on the reaction

$$2HONO \rightarrow H_2O + NO + NO_2 \quad (69)$$

using a variety of methods and comparing reactions between cis and trans HONO. The calculations were performed with B3LYP, QCISD(T), RCCSD(T) and G2M(RCC,MP2) methods using 6-311G(d,p) basis set. The study shows that the reaction occurs in two steps with a H_2O + ONONO intermediate. Furthermore, they have determined at least three parallel reaction paths via four-, five- and six-member ring transition states, with the four-member ring transition state contributing the least due to a significantly higher activation energy than the other two. The computed rate constants are orders of magnitude lower than experimental data, explained as heterogeneous effects on the experimental rate.

In a similar work, Lu et al. (2000) examined the reaction

$$HONO + HNO \rightarrow 2NO + H_2O \quad (70)$$

using the same methods and basis set. Note that this is stoichiometrically a more efficient way to generate NO than Equation (69). However, the barrier for this reaction is 88 kJ/mole and is much higher than that for the previous reaction and the conclusion is that this is kinetically less favorable than the previous reaction. However, the energetics of these reactions however may change in the presence of a catalyst, and thus the relative importance of the two reactions.

Certainly, there are numerous other MO-TST studies on atmospheric nitrogen oxide compound reactions. A number of these reactions relate to compounds that are combustion by-products such as HNO with •NO (Bunte et al.,1997), $\bullet NO_3$ with •H and $\bullet HO_2$ (Jitariu and Hirst 1998; 1999). Some seek to determine pathways to nitric acid, a component of acid rain (e.g., Boughton et al. 1997).

Greenhouse gas—methane. The temperature of the surface of the Earth is increasing (Jones et al. 1986), and this phenomenon is attributed to the increase in the amount of greenhouse gases (Mann and Park 1996). Among the greenhouse gases, methane is particularly important because it has been shown that the rate of increase in atmospheric methane is getting higher (Stevens and Engelkemeir 1988). This is notable since the absorption of radiation by methane is twenty times more effective than absorption by CO_2 in heating the troposphere (Turekian 1996). Pinpointing the sources of these gases has not been simple (Schoell 1980; Stevens and Engelkemeier 1988; Tyler 1992) and can be enormously aided by the use of isotopic signatures, in particular by the $\delta^{13}C$ and δD values of both the various sources and the atmospheric reservoir. By measuring the isotopic composition of atmospheric methane and comparing it to the isotopic composition of the sources, one can carry out a mass balance on the fluxes of the methane. However, the methane in the atmosphere is destroyed mainly by reactions with hydroxyl radicals,

$$CH_4 + \bullet OH \rightarrow \bullet CH_3 + H_2O \quad (71)$$

which leads to a residence time for methane of 10 years. This reaction changes the isotopic composition of the atmospheric methane. As a result, the application of isotopic tracers can only be made if the kinetic isotope effect of the reaction with hydroxyl radicals is known (Lasaga and Gibbs 1991). This kinetic isotope effect is critical and much effort has been spent to try to measure the effect experimentally and to obtain the temperature dependence (Rust and Stevens 1980; Davidson et al. 1987; Cantrell et al. 1990). Because •OH is so reactive and the methane reaction is slow, the experimental work has produced divergent results.

Conventional MO-TST studies have been performed on Equation (64) by numerous workers including Truong and Truhlar (1990), Lasaga and Gibbs (1991), Melissas and Truhlar (1993a), and Dobbs et al. (1993). Pertinent *ab initio* and experimental data have

been summarized in Table 3. All these studies calculated ZPE-corrected activation energies close to the upper limit of the experimental results.

Truong and Truhlar (1990) obtained initial transition state guesses drawn from a novel interpolation technique inspired by Hammond's postulate. These were subsequently optimized to true transition states. The calculations were performed to the MP-SAC2//MP2/6-311G(3d,2p) level. The rate constants were determined using TST and the zero theory interpolation model, wherein the rate constant is equal to the product of the TST rate constant and the zero-order interpolation of the zero-curvature ground

Table 3. Kinetic *ab initio* and experimental data for the reaction CH_4+•OH → CH_3+H_2O, showing activation energies and kinetic isotope effects. (See bottom for references.)

Zero-point corrected activation energies (kJ/mole)

Source	*TT*	*LG*	*MT*	*DO*	*DEx*
forward	27.6	27.5	24.7	21.9	8-25
backward	89.96		86.36		

Kinetic isotope effects (‰)

Source	*LG*	*MT*	*DAx*	*RSx*	*CAx*	*MT*
T(K)	k_{12}/k_{13} -1	k_{12}/k_{13} -1	k_{12}/k_{13} -1	k_{12}/k_{13} -1	k_{12}/k_{13} -1	k_{CH_4}/k_{CD_4}-1
150	3.6					
175	5.11					
200	6.1					
223		5.0				15.9
225	6.7					
250	7.1					
273		5.0			5.4	10.1
275	7.2				5.4	
293		5.0			5.4	8.7
298		5.0	10	3.0	5.4	8.39
300	7.3	5.0			5.4	8.27
325	7.2				5.4	
350	7.1				5.4	
353		5.0			5.4	6.0
400		5.0				4.82
416		5.0				4.53
800		3.0				2.16
1500		2.0				1.59
2400		1.0				1.45

References	*Theory*	*Method(+Basis set)*
(TT) Truong and Truhlar 1990	IVTST	MP-SAC2/6-311G(3d,2p)
(LG) Lasaga and Gibbs 1991	TST	MP2/6-311G(d,p)
(MT) Melissas and Truhlar 1993b	IVTST	MP-SAC//MP2/adj-cc-pVTZ
(DO) Dobbs et al. 1993		QCISD/CC
(DEx) DeMore et al. 1987		Experiment
(RSx) Rust and Stevens 1980		Experiment
(DAx) Davidson et al. 1987		Experiment
(CAx) Cantrell et al. 1990		Experiment

state (ZCG-0) transmission coefficient. Their study shows significant depression of the TST rate constants compared to experiment of up to two orders of magnitude in the temperature range 200-300 K; this is true despite considering tunneling corrections. On the other hand, the ZCG-0 results show the correct magnitude in the entire temperature range of the study, i.e., 200-2000 K.

Lasaga and Gibbs (1991) investigated kinetic isotope effects ($^{13}CH_4/^{12}CH_4$) of Equation (71) using TST and the Eckart tunneling correction (Johnston 1966). The predicted KIE values, in general, overestimate all the experimental values except that of Davidson et al. (1987). Related to this study, Xiao (unpublished results) performed a steepest descent calculation from the transition state (Fig. 9). These calculations of the minimum energy path are preliminaries needed for VTST calculations.

Melissas and Truhlar (1993a) studied the kinetic isotope effects (CD_4/CH_4) of Equation (71) using TST, CVT, and interpolated VTST (IVTST), which uses the small curvature tunneling (SCT) correction (Melissas and Truhlar 1993b). Their calculations show that accuracy of the KIE prediction increased dramatically from TST to IVTST.

Dobbs et al. (1993) determined the reaction coordinate of Equation (71) using very high levels of MO calculations. The zero point corrected activation energy at these levels of theory is the lowest determined (Table 3) and is well within the experimental range.

Acid rain—sulfur dioxide. Sulfur dioxide entering the atmosphere by direct anthropogenic input or by oxidation of biogenic sulfur bearing compounds is immediately oxidized to sulfate and is one of the main causes of acid rain. There is much interest in understanding the kinetic pathways that convert SO_2 to H_2SO_4. Two major mechanisms for the oxidation of SO_2 are homogeneous and heterogeneous oxidation, the latter occurring either by cloud scavenging of SO_2 or by oxidation on the surface of aerosols, which usually contain water. Tanaka et al. (1994) has succinctly described the different oxidation pathways of SO_2. The nature of the problem is as complicated as there are elementary reactions and species in the conversion. The reactions under scrutiny are for the homogenous reaction (Calvert et al. 1985; Margitan 1984; Anderson et al. 1989):

$$SO_2 + \bullet OH \rightarrow \bullet HOSO_2 \quad (72)$$

$$\bullet HOSO_2 + O_2 \rightarrow SO_3 + \bullet HO_2 \quad (73)$$

$$SO_3 + H_2O \rightarrow H_2SO_4 \quad (74)$$

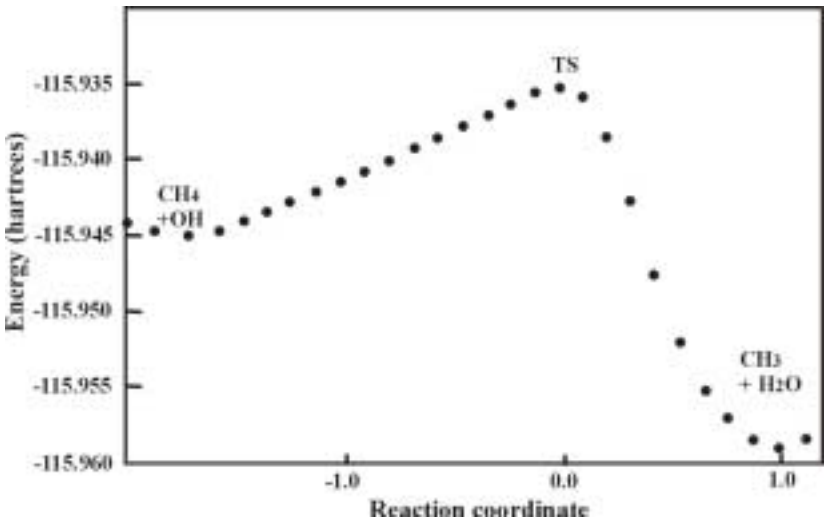

Figure 9. Steepest descent calculation from TS for the CH_4 + •OH system at MP2/6-311G(d,p).

and for the heterogeneous pathway

$$SO_{2(g)} \rightarrow SO_{2(aq)} \quad (75)$$

$$SO_{2(aq)} + H_2O \rightarrow HSO_3^- + H^+ \quad (76)$$

$$HSO_3^- + H_2O_2 \rightarrow SO_4^{2-} + H^+ + H_2O \quad (77)$$

Both reaction pathways have been extensively studied in controlled laboratory experiments in order to identify major reactions and their rate constants. The quantification of the relative importance of these two pathways in natural environments is, however, very difficult and controversial. MO-TST provides an additional means to determine the kinetics of these reactions.

The understanding of the homogeneous pathway is far from complete. Anderson et al. (1989) considers Equation (72) as the slow, rate determining reaction and has been observed to occur experimentally (e.g., Egsgaard et al. 1988). Tanaka et al. (1994) have determined the reaction coordinate for this mechanism using constrained optimization and have computed the kinetic isotope effects.

The formation of SO_3 from $HOSO_2$ has been indirectly observed experimentally (e.g., Gleason et al. 1987) and the results indicate that Equation (70) is a fast reaction. The reaction coordinate has been computed by Majumdar et al. (2000) using B3LYP with 6-31G(d,p), triple-, quadruple- and quintuple-zeta basis sets with diffuse basis functions.

Equation (74) has received the most experimental (e.g., Kolb et al. 1994; Brown et al. 1996) and theoretical attention. The gas-phase reaction probably involves the initial formation of a SO_3-H_2O complex, which subsequently formed H_2SO_4. Hofmann and Schleyer (1994) have carried out a careful study of the reaction at the MP4/6-311+G(2df,p)//MP2/6-31+G(d) level and have calculated a barrier for conversion of 115 kJ/mole. Morokuma and Muguruma (1994) gave theoretical support to the conversion of SO_3 to H_2SO_4 with the catalytic effect of an additional water molecule. This is significant, since the assumed homogenous overall reaction may in fact involve a step that proceeds faster as a heterogeneous reaction. Catalysis facilitated by a proton does not occur in this reaction, as observed by Pommerening et al. (1999) in a combined experimental and *ab initio* study.

The main problem with the heterogeneous pathway is that sulfurous acid, H_2SO_3 has not been isolated yet. The experimental analyses of aqueous solutions (Davis and Klauber 1975) suggest that H_2SO_3 is a loosely aquated SO_2 molecule and some have reported on the relative stability of the bisulfite $HOSO_2^-$ and sulfonate HSO_3^- ions (Brown and Barber 1995; Vincent et al. 1997). Any modeling of the heterogeneous pathway should be consistent or explain this elusiveness of H_2SO_3 or HSO_3^-.

The solvation of SO_2 has been studied experimentally (Matsumura et al. 1989; Schriver et al. 1991) and theoretically although the picture is not yet complete. Bishenden and Donaldson (1998), and Li and McKee (1997) studied both Equations (75) and (76) using two different methods to simulate the aqueous phase reaction. Bishenden and Donaldson used a dielectric continuum model with only one water molecule in the system whereas Li snd McKee (1997) had an additional second “spectator” water molecule. The formation of the solvated SO_2 is weakly exothermic (-5.9 kJ/mole) and favored according to Bishenden and Donaldson (1998), although they did not calculate any transition state for Equation (75). The weak binding energy is enhanced by additional hydrogen bonds from the spectator water molecule, according to Li and McKee. Both studies showed that Equation (76) has a high positive free energy change and a large activation energy barrier with the small systems used. The lower activation energy with

an additional water molecule calculated by Li and McKee (1997) supports the view that this is indeed a heterogeneous reaction catalyzed by water molecules.

ACCURACY ISSUES

Basis sets

We mentioned in the discussion on calculating the PES from MO theory that the infinite basis electronic wavefunction $\mathbf{\Phi}$ was approximated by a finite basis set wavefunction $\mathbf{\Phi'}$. The wavefunction $\mathbf{\Phi'}$ may be, as another layer of approximation, separated into a product of functions dependent only on coordinates of a single electron. These single electron coordinate functions are called "molecular orbitals" Ψ_i and may be approximated by a linear combination of "atomic orbitals" (LCAO), thus

$$\Psi_i = \sum_j^N c_{ji}\varphi_j \tag{78}$$

where φ_j, are the atomic orbitals. The physical interpretation of the LCAO approach is that the molecular orbital is assumed to be composed of the sum of atomic orbitals (hence the phrase, "atoms in molecules"). The set of atomic orbitals used for constructing a molecular orbital is called the "basis set." These atomic orbitals are often Slater-type orbitals (characterized by an exponential factor $e^{-\xi r}$, where ξ is a coefficient) or themselves linear combinations of functions called "primitives", which are almost always gaussian-type orbitals (g_k, characterized by an exponential factor $e^{-\xi r^2}$).

$$\varphi_j = \sum_k^M d_{kj} g_k \tag{79}$$

The ideal choice for a good atomic orbital basis set is one that produces the correct behavior at the critical regions, i.e., on the nuclear positions and in the outer regions. Although Slater orbitals produce the desired characteristics naturally, gaussian-type primitives are preferred due to their ease in integral evaluations. When the gaussian coefficients and exponents are pre-determined, the sets of atomic orbitals are called "contracted basis sets." The use of gaussian-type primitives introduces yet another layer of approximation.

All these approximations introduce errors and minimizing these errors is a major goal in any calculation of the PES. As a general rule, the larger the basis set used, the more accurate (and expensive) the calculations. Note that the "atoms in molecules" approximation is insufficient for a realistic representation since atoms are expected to be significantly modified in a molecule. Additional functions can be incorporated in φ to emphasize specific characteristics of the electron cloud. Polarization functions (Frisch et al. 1984) may be added when one expects displacements of the centers of electron density from the nuclear centers (e.g., Sordo 2000). Diffuse functions (Clark et al. 1983) may be added if one expects the charge distribution to be more diffuse than in the neutral atom (e.g., Glukhovtsev 1995; Alagona and Ghio 1990) for example in anions.

Choosing a basis set depends on the type of system being studied and the method being used (e.g., Bauschilder and Partridge 1998; Tsuzuki et al. 1996). Grüneich and Hess (1998) recommend several guidelines on choosing gaussian-type basis sets for periodic MO calculations.

Basis-set effects testing is rather routine in most MO studies. Furthermore, new types of basis-sets are actively being developed and introduced (e.g., de Castro and Jorge 1998; Mitin et al. 1996) and therefore accuracy comparisons and calibrations regularly

need to be done. There are numerous studies on the basis-set effects on electron charge distributions (Tsuzuki et al. 1996; Nath et al. 1994; Alkorta et al. 1993), reaction energies (Bak et al. 2000; Bauschilder and Partridge 1998; Delbene and Shavitt 1994; Cybulski et al. 1990) and electronegativities (Nath et al. 1993). Investigations on systems relevant to the geosciences are numerous as well. There are several recent studies of the basis-set effects in the chemical properties of systems of water (Maroulis 1998; Papadopoulos and Waite 1991) and hydrogen bonded systems (Tschumper et al. 1999; Tsuzuki et al. 1999). Kubicki et al. (1995) examined the changes in geometries, charge distributions, and vibrational spectra of free silica and alumina and their anions. Bar and Sauer (1994) studied the basis-set effects of configurations and chemical properties of systems of silica and Nicholas et al. (1992) on zeolites. Zinc oxide and zinc sulfide chemical properties were investigated by Martins et al. (1995) and Muilu and Pakkanen (1994). Tsuzuki et al. (1994) and Schultz and Stechel (1998) investigated basis-set effects on the properties of organic compounds relevant to hydrocarbon generation. There are also numerous studies on the chemical properties of atmospheric species (e.g., Xenides and Maroulis 2000). There are only a few basis-set effect studies addressing MO-TST, among them the work of Pan and McAllister (1998), Glad and Jensen (1996) and Glidewell and Thompson (1984).

Basis set superposition error

Basis set superposition error (BSSE) occurs when the basis set used to compute the energy of the reacting complex is bigger than the basis set used for computing the energy of the individual reactants. It was found that BSSE would not be a problem if the basis sets were sufficiently large (Martin et al. 1989). The error is of particular concern with gas-phase reactions where one considers infinite separation before a reaction. With condensed states, the BSSE may be avoided even with smaller basis sets because in reality the molecules are never infinitely separated from the surrounding environment and therefore, in principle, one can use the same stoichiometry (and basis) for the reactant and transition state configurations.

There are three suggested ways to correct the error: the Boys and Bernardi (1970) counterpoise method (CP), the chemical Hamiltonian approach (CHA) (Mayer 1983), and the local correlation method (Saebo et al. 1993). In the CP method, which is the more popular method, the individual reactants are recomputed using the reacting complex basis set by introducing ghost atoms. This method has not been without controversy (Liedl 1998; van Duijneveldt 1997; Turi and Dannenberg 1993; references within). In the CHA scheme, one attempts to get rid of the energy in the reacting complex when determining the wavefunction by omitting terms in the Hamiltonian which contribute to the BSSE. Recent investigations on the merits of this scheme have been done by several workers (Halasz et al. 1999; Paizs and Suhai 1997; Valiron et al. 1993).

There are many studies on the BSSE. For example, Simon et al. (1999) studied BSSE in systems of water molecules. Investigations of BSSE on hydrogen bonding were conducted by Simon et al. (1996) and Alagona and Ghio (1995). Fuentealba and Simon-Manso (1999) discuss BSSE in atomic clusters.

Methods

Another factor affecting the accuracy of the calculations is the choice of MO methods used to generate the reaction coordinates. Tossell and Vaughan (1992) provide an excellent and thorough discussion of methods as well as their applications to materials relevant to the geosciences. Among the *ab initio* approaches, the Hartree-Fock or HF method (Blinder 1965) has traditionally been the starting point for developing more accurate methods. The inadequacy of the HF method lies in its insufficient handling of

electron correlation. Configuration interaction methods (Schaefer 1972) and perturbation schemes to improve on HF results, such as Moller-Plesset (MP) methods (Moller and Plesset 1934), attempt to correct for electron correlation. The drawback of most of these improvements to HF is the computational cost.

Lately, density functional theory or DFT, which is based on the work of Hohenberg and Kohn (1964), has become popular because it is less expensive and handles both electron and exchange correlation satisfactorily. DFT is not one method, but a class of methods that calculate the total electronic energy as a functional of the electron density following the work of Kohn and Sham (1965).

There can be no cross calculations between the methods, meaning one cannot, for example, take the difference of energies of a minimum calculated by HF and a transition state from a DFT method to obtain an activation energy. Doing so would produce bizarre results. As with the choice of basis sets, one needs to make a decision depending on the merits and appropriateness of the methods on the particular system in consideration.

Johnson (1994) investigated the performance of different DFT methods. With materials important to the geosciences, Xantheas (1995) and Simon et al. (1999) have compared methods on water clusters, Harris et al. (1997) on iron hydrates, and Bacelo and Ishikawa (1998) on sodium hydrates. Gas phase acidities were investigated by Smith and Radom (1995). Recently, Bak et al. (2000) compared the accuracy in reaction enthalpies and atomization energies of different small systems using several methods and basis sets.

MO-TST studies often include comparisons of reaction curves using several methods as well as basis sets (e.g., Xiao and Lasaga 1996).

Long-range interactions

Accounting for all the significant contributions in the reaction environment is a major goal for reaction modeling. Long-range interactions may be significant in condensed states. As mentioned earlier, one may take a periodic approach to a solid phase problem. In the case of a finite approach, one has to determine a good cluster size, and embedding clusters may be worthwhile to investigate.

For reactions in solution, one may implement explicit or implicit hydration schemes. In explicit hydration, water molecules are included in the system. These additional water molecules have a significant effect on the reaction coordinates of a reaction (e.g., Felipe et al. 2001). Implicit hydration schemes, or dielectric continuum solvation models (see Cramer and Truhlar 1994), refer to one of several available methods. One may choose between an Onsager-type model (Wong et al. 1991), a Tomasi-type model (Miertus et al. 1981; Cancès et al. 1997), a "static isodensity surface polarized continuum model" or a "self consistent isodensity polarized continuum model" (see Frisch et al. 1998).

Dissolution reactions, for example, need to take into account the surrounding water molecules. In conventional MO-TST, one may use larger clusters and any of the two hydration schemes. An alternative is a periodic "slab" to model a crystal surface, explicitly adorned with water molecules and optionally given an implicit hydration treatment. The significance of applying these continuum solvation methods on MO-TST studies has not been well established in geochemistry.

Activation energies and zero point energies

The activation energy has been the most widely used measure to determine the merits of a proposed reaction mechanism. Through appropriate consideration of the reacting system and environment, activation energies reasonably close to empirically

measured ones have been computed for a number of cases. However, one should be cautious about the validity of this measure. Condensed and heterogeneous systems for instance allow a certain degree of ambiguity in defining a reaction (Truhlar et al. 1996). For example, the rate of a reaction is expected to be a statistical result of several similar reactions (Dellago et al. 1998). These reactions can have comparable barrier heights but have different temperature dependencies. Thus a single MO-TST mechanism may not reproduce the empirically determined temperature dependence of the rate constant, despite it being a valid mechanism for the particular reaction. In other words, there may be other pathways that lead from products to reactants, and the actual reaction may be a result of several parallel reactions. Truhlar et al. (1996) have documented recent advances and extensions of TST to condensed phase reactions.

Although reasonable activation energies may be obtained, it is still often difficult to predict accurate thermal rate constants. One reason for this is the deviation of the real system from ideality, which introduces parameters that are not computationally well-defined in the conventional MO-TST approach. Recall that the quasi-equilibrium constant in Equation (6) is in terms of activities. Thus, the rate constant equation (Eqn. 12) is a function of activity coefficients of reactants and transition states, and these coefficients cannot be computed with the usual Debye-Huckel model.

A common error committed is the neglect of ZPE in an evaluation of reaction feasibility. While energy differences where ZPE is not considered are occasionally helpful in qualitatively determining whether the hypothesized reaction produces the expected rate, the ZPE should unequivocally be considered in any quantitative TST evaluation of reaction rates.

Quantum tunneling

Tunneling occurs when a configuration, that has an energy lower than an energy barrier, nonetheless surmounts it due to quantum mechanical effects. In such cases, adjustments of the rate constant due to tunneling become necessary to obtain improved accuracy. These corrections in TST and VTST are in the form of a correction coefficient κ such that

$$k_{r,corr} = \kappa k_r \tag{80}$$

where $k_{r,corr}$ is the corrected rate constant. (Note that quantum effects are incorporated in the semi-classical rate theories TST and VTST in an *ad hoc* fashion.) In general, reaction mechanisms where small masses are involved require tunneling corrections. Thus mechanisms where hydrogen atoms are the primary elements involved need to be corrected for tunneling.

In the first order Wigner treatment (see Truhlar et al. 1985), which is the most common correction made, the coefficient is given by

$$\kappa = 1 + \frac{1}{24}\left|\frac{h\nu^{\ddagger}}{2\pi kT}\right|^2 \tag{81}$$

where $\nu^{\ddagger}$ is the imaginary vibrational frequency at the saddle point. However, this correction is only valid if certain conditions are satisfied. First, the contributions to tunneling must only come from the saddle point region of the PES where transverse modes do not vary appreciably. The PES curvature should also be that of a concave down parabola. The Wigner correction is considered valid only at very high temperatures where it is near unity.

Alternative corrections are Eckart tunneling, multidimensional zero-curvature tunneling, and multidimensional small-curvature tunneling (Truhlar et al. 1982), in increasing order of accuracy. The last two involve points on the PES other than the first order saddle point and have more sophisticated calculations.

CONCLUSIONS AND FUTURE DIRECTIONS

MO theory when used in conjunction with TST offers a method to calculate rate constants that complements experimental methods. Lately, MO theory has benefited from the advances in computer technology and as a result, opportunities for testing long held formulations in TST have opened. This has also invigorated development of other rate theories where data from MO calculations may be used. In particular, rapid growth in the field of VTST is making possible the computation of even more accurate rate constants than those given by TST.

An advantage of MO-TST over experimental work is the elucidation of atomic scale processes. The direct physical observation of a reaction in the atomic scale cannot be done without perturbing the system due to the Heisenberg uncertainty principle. MO-TST makes possible the "observing" of the progress of a reaction, albeit virtual, with the system remaining undisturbed. "Snapshots" at different points of the reaction progress can be taken to create an animation of the reaction. While it should be emphasized that the real reaction proceeds through several different paths, the visual depiction of a possible path is both informative and educational, aiding the intuitive understanding of the chemical behavior of a system.

The emphasis of MO-TST work on condensed phases in the geosciences has been primarily on weathering and dissolution reactions. While these have produced insightful results and have encouraged other studies, isotope exchange reactions have more experimental data that can be used to test and calibrate the MO-TST approach. Frequently, the PES of isotope exchange reactions is easier to probe than weathering and dissolution reactions because, in the former, the molecular subgroups affected by the reaction are often smaller and thus there are fewer modes where configurational changes occur. The computational time difference in finding reasonable transition state guesses is significant. Thus, we suggest tackling the generally simpler problem of isotope exchange reactions first, particularly those occurring in solution, before addressing the more difficult problem of dissolution.

Among the main future thrusts in research is the investigation of larger systems. The major difficulty encountered as the size of the system grows is the increased computational complexity in MO calculations. Specifically, the computational effort typically increases exponentially with the number of electrons in the system. To ameliorate this, one may use mixed basis sets: large basis sets are used for the inner active zone where the reaction actually occurs and smaller basis sets are used for atoms in the outer zones. This technique reserves the more accurate but tedious calculations for regions where they are most needed and implements less expensive calculations for less critical regions. Mixed basis set calculations can be performed in some commercially available programs (e.g., Frisch et al. 1998). In addition, methods that combine expensive quantum mechanical methods with cheaper molecular mechanical methods are being developed. An example of this is the "Our own N-layered Integrated molecular Orbital molecular Mechanics" (ONIOM) method (Dapprich et al. 1999). In ONIOM, the system is subdivided into physical layers, and an application of a high and expensive level of approximation is given to the first layer where the bond formation and breaking occurs, and application of progressively lower and less expensive levels are given to the other

layers. Hence, the ONIOM method is at the core (literally speaking) an MO approach and data obtained from it being used in MO-TST work is a welcome prospect. ONIOM has been applied to the determination of reaction coordinates of different systems such as organometallic reactions (Cui et al. 1998), enzymatic reaction processes (Froese et al. 1998), and photodissociation reactions (Cui et al. 1997).

Periodic MO-TST methods offer another promising direction in studying larger systems particularly those involving heterogeneous phases. Related to this is the procedure of embedding clusters (Pisani and Ricca 1980). There have been many studies using these methods to determine equilibrium configurations and properties (e.g., Civalleri et al. 1999). However, there are only a few examples to elucidate transition states and reaction rates, and there are even fewer studies on geochemically relevant systems.

The problem of increasing computational complexity with system size ultimately originates from the numerical approximation of the Schrödinger equation (Eqn. 21). A recent active area in the field of computational quantum mechanics is the development of linear-scaling electronic structure schemes (so-called "$O(N)$ methods") where, for example, certain features of the matrices arising from the numerical approximation are exploited. Galli (2000), Goedecker (1999) and Ordejon (1998) review such methods proposed by several groups. The impact of these on future MO-TST studies is expected to be significant.

ACKNOWLEDGMENTS

This work was supported by the National Science Foundation (NSF EAR 9628238) and the Office of Naval Research. The authors would like to thank two anonymous reviewers and Randy Cygan for their insightful comments, intelligent suggestions and careful editing. The authors would like to thank A. E. Bence for reviewing the contents of the manuscript.

LIST OF SYMBOLS

$\in$	rational functional
ε_{ej}	jth electronic energy
ε_{nj}	jth nuclear energy
ε_{o}	zero-point energy
κ	correction coefficient for quantum effects
λ	shift parameter; also wavelength; also eigenvalue (with subscript)
$\nu^{\ddagger}$	transition state unimolecular frequency of conversion; also vibrational frequency at saddle point
ν_j	jth vibrational mode; also orthonormal eigenvector
φ_j	jth atomic orbital
σ	symmetry number
τ	average lifetime of transition state
$\mathbf{\Phi}$	electronic wavefunction
$\mathbf{\Phi'}$	electronic finite-basis wavefunction
$\boldsymbol{\chi}$	nuclear wavefunction
χ_{r}	characteristic function of the reaction
$\mathbf{\Psi}$	time-independent wavefunction solution to Schrödinger equation
Ψ_i	ith molecular orbital
ω_{ej}	degeneracy of jth electronic state
ω_i	angular frequency

ω_{nj}	degeneracy of jth nuclear state
E, E_{tot}	energy
E_{el}	electronic potential energy
$\mathbf{F}$	mass-weighted force constant matrix
F	flux
F	degrees of freedom
f	dividing surface separating "reactants" from "products"; also interpolation parameter
G	gradient
$\Delta G_C^{\ddagger gen}$	CVT generalized free energy of activation
g_k	kth gaussian-type orbital
$\mathbf{H}$	Hamiltonian
H	Hessian
h	Heaviside function, $\mathrm{h}[x] = \{1$ for $x > 0$, ½ for 0, 0 for $x < 0\}$
h	Planck's constant
I	identity matrix; also moment of inertia
I_{x}, I_{y}, I_{z}	principal moments of inertia
J	total angular momentum
$K^{\ddagger}$	quasi-equilibrium constant
K^{o}	reaction quotient evaluated at the standard state
K_{eq}	equilibrium constant
k	Boltzmann's constant
k_{r}	reaction rate constant
$k_{\text{r}}^{\text{CVT}}$, $k_{\text{r}}^{\text{gen}}$	CVT generalized rate constant
$k_{r,corr}$	reaction rate constant corrected for quantum effects
l	predetermined step size
m, m_i	mass
N	number of nuclear centers
$N(E)$	cumulative reaction probability
n_p	final quantum state of the product molecules
n_r	initial quantum state of the reactant molecules
$\mathbf{p}$	momentum
p	path coordinate
Q	generalized partition function
$Q^{\updownarrow}$	generalized transition state molecular partition function without imaginary vibrational component
$Q_C^{\ddagger gen}$	CVT generalized transition state partition function
Q_{R}	generalized reactant partition function
Q_r	quantum mechanical reactant partition function per unit volume
$\mathbf{q}$	coordinates
$\mathbf{q}(t)$	classical trajectory
$q^{\updownarrow}$	transition state molecular partition function without imaginary vibrational component
q_i	ith molecular partition function
q_{transl}	molecular partition function composed of imaginary vibration
$\mathbf{R}$	nuclear coordinate matrix
R	universal gas constant
$\mathbf{r}$	electronic coordinates
$\mathbf{r}_i$	atomic coordinates of ith atom
r_{ab}	internuclear distance between atoms a and b
r_R	reactant internuclear distances
r_P	product internuclear distances

S	symmetric scaling matrix
S_{n_P,n_r}	S-matrix
s	reaction coordinate; also step size
s_c^{CVT}	reaction coordinate at the CVT divide
T	temperature
$\mathbf{T}_{\mathrm{el}}$	electronic kinetic energy operator
$\mathbf{T}_{\mathrm{n}}$	nuclear kinetic energy operator
T_{n}	nuclear kinetic energy
V	molecular volume
$\mathbf{V}_{\mathrm{ee}}$	interelectronic potential energy operator
$\mathbf{V}_{\mathrm{ne}}$	nucleus-electron potential energy operator
$\mathbf{V}_{\mathrm{nn}}$	internuclear potential energy operator
V_{nn}	internuclear potential energy
V_{s}	potential energy surface
$\mathbf{x}_k$	kth mass-weighted position vector
$\mathbf{y}_i$	ith linearly-independent normal modes

REFERENCES

Alagona G, Ghio C (1995) Basis-set superposition errors for Slater vs gaussian-basis functions in H-bond interactions. Theochem-J Mol Struc 330:77-83

Alagona G, Ghio C (1990) The effect of diffuse functions on minimal basis set superposition errors for H-bonded dimers. J Comput Chem 11:930-942

Alkorta I, Villar Ho, Perez JJ (1993) Effect of the basis-set on the computation of molecular-polarization. J Phys Chem 97:9113-9119

Amos RD, Alberts IL, Andrews JS, Colwell SM, Handy NC, Jayatilaka D, Knowles PJ, Kobayashi R, Laidig KE, Laming G, Lee Am, Maslen PE, Murray CW, Rice JE, Simandiras ED, Stone AJ, Su MD, Tozer DJ (1995) The Cambridge Analytic Derivatives Package Issue 6. Cambridge University, Cambridge, UK

Anderson LG, Gates PM, Nold CR (1989) Mechanism of atmospheric oxidation of sulfur-dioxide by hydroxyl radicals. ACS Sym Ser 393:437-449

Atabek O, Miretartes S, Jacon M (1985) 3-dimensional quantum calculation of the vibrational-energy levels of ozone. J Chem Phys 83:1769-1777

Ayala PY, Schlegel HB (1997) A combined method for determining reaction paths, minima and transition state geometries. J Chem Phys 107:375-384

Bacelo D, Ishikawa Y (1998) Comparison of density functional and MP2 geometry optimizations of $Na(H_2O)(n)$ (n = 1-3) clusters. Theochem-J Mol Struc 425:87-94

Badro J, Teter DM, Downs RT, Gillet P, Hemley RJ, Barrat JL (1997) Theoretical study of a five-coordinated silica polymorph. Phys Rev-B 56:5797-5806

Bak KL, Jorgensen P, Olsen J, Helgaker, T, Klopper W (2000) Accuracy of atomization energies and reaction enthalpies in standard and extrapolated electronic wave function/basis set calculations. J Chem Phys 112:9229-9242

Baker J (1986) An algorithm for the location of transition states. J Comp Chem 7:385-395

Baker J (1987) An algorithm for geometry optimization without analytical gradients. J Comp Chem 8:563-574

Banerjee A, Adams N, Simons J, Shepard R (1985) Search for stationary points on surfaces. J Phys Chem 89:52-57

Bar MR, Sauer J (1994) *Ab initio* calculations of the structure and properties of disiloxane. The effect of electron correlation and basis-set extension. Chem Phys Lett 226:405-412

Baulch DL, Cox RA, Crutzen PJ, Hampson RF, Kerr JA, Troe J, Watson RT (1982) Evaluated kinetic and photochemical data for atmospheric chemistry 1. Codata task group on chemical kinetics. J Phys Chem Ref Data 11:327-496

Bauschilcher CW, Partridge H (1998) The sensitivity of B3LYP atomization energies to the basis set and a comparison of basis set requirements for CCSD(T) and B3LYP. Chem Phys Lett 287:216-216

Bernal JD, Fowler RH (1933) A theory of water and ionic solution, with particular reference to hydrogen and hydroxyl ions. J Chem Phys 1:515-548

Bianco R, Hynes JT (1999) A theoretical study of the reaction of $ClONO_2$ with HCl on ice. J Phys Chem A 103:3797-3801

Bishenden E, Donaldson DJ (1998) *Ab initio* study of SO_2+H_2O. J Phys Chem A 102:4638-4642
Blinder, SM (1965) Basic concepts of self-consistent-field theory. Am J Phys 33:431-443
Boughton JW, Kristyan S, Lin MC (1997) Theoretical study of the reaction of hydrogen with nitric acid: *Ab initio* MO and TST/RRKM calculations. Chem Phys 214:219-227
Boys SF, Bernardi F (1970) Calculation of small molecular interactions by differences of separate total energies—some procedures with reduced errors. Mol Phys 19:553-566
Brown RC, MiakeLye RC, Anderson MR, Kolb CE (1996) Effect of aircraft exhaust sulfur emissions on near field plume aerosols. Geophys Res Lett 23:3607-3610
Brown RE, Barber F (1995) *Ab initio* studies of the thermochemistry of the bisulfite and the sulfonate ions and related-compounds. J Phys Chem 99:8071-8075
Brune WH, Anderson JG, Toohey DW, Fahey DW, Kawa SR, Jones RL, Mckenna DS, Poole LR (1991) The potential for ozone depletion in the arctic polar stratosphere. Science 252:1260-1266
Bunte SW, Rice BM, Chabalowski CF (1997) An *ab initio* QCISD study of the potential energy surface for the reaction HNO+NO→N_2O+OH. J Phys Chem A 101:9430-9438
Calvert JG, Chatfield RB, Delany AC, Martel EA (1985) Evidence for short SO_2 lifetimes in the atmosphere—an *in situ* measurement of atmospheric SO_2 lifetime using cosmic-ray produced s-38. Atmos Environ 19:1205-1206
Cancès E, Mennucci B, Tomasi J (1997) A new integral equation formalism for the polarizable continuum model: Theoretical background and applications to isotropic and anisotropic dielectrics. J Chem Phys 107:3032-3041
Cantrell CA, Shetter RE, McDaniel AH, Calvert JG, Davidson JA, Lowe DC, Tyler SC, Cicerone RJ, Greenberg JP (1990) Carbon kinetic isotope effect in the oxidation of methane by the hydroxyl radical. J Geophys Res-Atmos 95:22455-22462
Casey WH, Lasaga AC, Gibbs GV (1990) Mechanisms of silica dissolution as inferred from the kinetic isotope effect. Geochim Cosmochim Acta 54:3369-3378
Casey WH, Sposito G (1992) On the temperature dependence of mineral dissolution rates. Geochim Cosmochim Acta 56:3825-3830
Cerjan CJ, Miller WH (1981) On finding transition states. J Chem Phys 75:2800-2807
Chapman S (1930) A theory of upper-atmosphere ozone. Mem Roy Meteorol Soc 3:103
Civalleri B, Casassa S, Garrone E, Pisani C, Ugliengo, P (1999) Quantum mechanical *ab initio* characterization of a simple periodic model of the silica surface. J Phys Chem B 103:2165-2171
Clark T, Chandrasekhar J, Spitznagel GW, Schleyer PV (1983) Efficient diffuse function-augmented basis-sets for anion calculations 3. The 3-21+G basis set for 1st-row elements, Li-F. J Comp Chem 4:294-301
Cramer CJ, Truhlar DG (1994) Structure and reactivity in aqueous-solution—an overview. ACS Sym Ser 568:1-7
Cui Q, Musaev DG, Morokuma K (1998) Molecular orbital study of H_2 and CH_4 activation on small metal clusters. II. Pd_3 and Pt_3. J Phys Chem 102:6373-6384
Cui Q, Morokuma K (1997) *Ab initio* MO studies on the photodissociation of C_2H_2 from the S_1 (^1A_u) state. II. Mechanism involving triplet states. Chem Phys Lett 272:319-327
Cybulski SM, Chalasinski G, Moszynski R (1990) On decomposition of 2nd-order Moller-Plesset supermolecular interaction energy and basis set effects. J Chem Phys 92:4357-4363
Czerminski R, Elber R (1990) Reaction-path study of conformational transitions in flexible systems—application to peptides. J Chem Phys 92:5580-5601
Dapprich S, Komaromi I, Byun KS, Morokuma K, Frisch MJ (1999) A new ONIOM implementation in Gaussian98. Part I. The calculation of energies, gradients, vibrational frequencies and electric field derivatives. Theochem-J Mol Struc 462:1-21
Davidson N (1962) Statistical Mechanics. McGraw-Hill, New York
Davidson JA, Cantrell CA, Tyler SC, Shetter RE, Cicerone RJ, Calvert JG (1987) Carbon kinetic isotope effect in the reaction of CH_4 with HO. J Geophys Res 92:2195-2199
Davis DD, Klauber G (1975) Atmospheric gas-phase oxidation mechanisms for molecule SO_2. Int J Chem Kinet 7:543-556
de Castro EVR, Jorge FE (1998) Accurate universal gaussian basis set for all atoms of the periodic table. J Chem Phys 108:5225-5229
Delbene JE, Shavitt I (1994) Basis-set effects on computed acid-base interaction energies using the dunning correlation-consistent polarized split-valence basis-sets. Theochem-J Mol Struc 113:27-34
Dellago C, Bolhuis PG, Csajka FS, Chandler D (1998) Transition path sampling and the calculation of rate constants. J Chem Phys 108:1964-1977
Demiralp E, Cagin T, Goddard WA (1999) Morse stretch potential charge equilibrium force field for ceramics: Application to the quartz-stishovite phase transition and to silica glass. Phys Rev Let 82:1708-1711

DeMore WB, Sander SP, Golden DM, Hampson, RF, Kurylo MJ, Howard CJ, Ravishankara AR, Kolb CE, Molina MJ (1992) Chemical kinetics and photochemical data for use in stratospheric modeling. Evaluation No 10 NASA, Jet Propulsion Laboratory Publ 92-20

Dennis JE Jr, Schnabel RB (1983) Numerical Methods for Unconstrained Optimization and Nonlinear Equations. Prentice-Hall, New Jersey, 378 pp

Dewar MJS, Healy EF, Stewart JJP (1984) Location of transition states in reaction-mechanisms. J Chem Soc-Faraday Trans 80:227-233

Dobbs KD, Dixon DA, Komornicki A (1993) *Ab initio* prediction of the barrier height for abstraction of H from CH_4 by OH. J Chem Phys 98:8852-8858

Doll JD, Voter AF (1987) Recent developments in the theory of surface-diffusion. Annu Rev Phys Chem 38:413-431

Eckert F, Werner HJ (1998) Reaction path following by quadratic steepest descent. Theor Chem Acc 100:21-30

Egsgaard H, Carlsen L, Florencio H, Drewello T, Schwarz H (1988) Experimental-evidence for the gaseous HSO_3 radical—the key intermediate in the oxidation of SO_2 in the atmosphere. Chem Phys Lett 148:537-540

Eyring H (1935a) The activated complex in chemical reactions. J Chem Phys 3:107-120

Eyring, H (1935b) The activated complex and the absolute rate of chemical reactions. Chem Rev 17:65-82

Farman JC, Gardiner BG, Shanklin JD (1985) Large losses of total ozone in Antarctica reveal seasonal ClO_x/NO_x interaction. Nature 315:207-210

Felipe MA, Kubicki JD, Rye DM (2001) Hydrogen isotope exchange kinetics between water and dissolved silica from *ab initio* calculations. Geochim Cosmochim Acta, submitted

Fermann JT, Blanco C, Auerbach S (2000) Modeling proton mobility in acidic zeolite clusters. I. Convergence of transition state parameters from quantum chemistry. J Chem Phys 112:6779-6786

Fleisher MB, Golender LO, Shimanskaya MV (1992) On the mechanism of water dissociation on the surface of Al_2O_3 quantum-chemical calculations. React Kinet Catal L 46:173-178

Fletcher R (1987) Practical Methods of Optimization. Wiley, Chichester

Fletcher R, Powell MJD (1963) A rapidly convergent descent method for minimization. Comput J 6:163-168

Fogarasi G, Zhou X, Taylor P, Pulay P (1992) The calculation of *ab initio* molecular geometries - efficient optimization by natural internal coordinates and empirical correction by offset forces. J Am Chem Soc 114:8191-8201

Foresman JB, Frisch A (1996) Exploring Chemistry with Electronic Structure Methods, 2nd ed. Gaussian Inc, Pittsburgh

Frisch MJ, Pople JA, Binkley JS (1984) Self-consistent molecular-orbital methods 25. Supplementary functions for gaussian-basis sets. J Chem Phys 80:3265-3269

Frisch MJ, Trucks GW, Schlegel HB, Scuseria GE, Robb MA, Cheeseman JR, Zakrzewski VG, Montgomery JA, Stratmann RE, Burant JC, Dapprich S, Millam JM, Daniels AD, Kudin KN, Strain MC, Farkas O, Tomasi J, Barone V, Cossi M, Cammi R, Mennucci B, Pomelli C, Adamo C, Clifford S, Ochterski J, Petersson GA, Ayala PY, Cui Q, Morokuma K, Malick DK, Rabuck AD, Raghavachari K, Foresman JB, Cioslowski J, Ortiz JV, Stefanov BB, Liu G, Liashenko A, Piskorz P, Komaromi I, Gomperts R, Martin RL, Fox DJ, Keith T, Al-Laham MA, Peng CY, Nanayakkara A, Gonzalez C, Challacombe M, Gill PMW, Johnson BG, Chen W, Wong MW, Andres J, Head-Gordon M, Replogle ES, Pople JA (1998) Gaussian 98 (Revision A7). Gaussian, Inc., Pittsburgh, PA

Froese RDJ, Musaev DG, Morokuma K (1998) A theoretical study of substituent effects in the diimine-M(II) catalyzed ethylene polymerization reaction using the IMOMM method. J Am Chem Soc 120:1581-1587

Fuentealba P, Simon-Manso Y (1999) Basis set superposition error in atomic cluster calculations. Chem Phys Lett 314:108-113

Fukui K (1981) The path of chemical reactions—the IRC approach. Acc Chem Res 14:363-368

Galli G (2000) Large-scale electronic structure calculations using linear scaling methods. Phys Status Solidi B 217:231-249

Garrett BC, Truhlar DG (1979) Generalized transition state theory. Bond-energy bond order method for canonical variational calculations with applications to hyrdogen atom transfer reactions. J Am Chem Soc 101:4534

Gibbs GV, Rosso KM, Teter DM, Boisen MB, Bukowinski MST (1999) Model structures and properties of the electron density distribution for low quartz at pressure: a study of the SiO bond. J Mol Struc 486:13-25

Glad SS, Jensen F (1996) Basis set and correlation effects on transition state geometries and kinetic isotope effects. J Phys Chem 100:16892-16898

Glasstone S, Laidler K, Eyring H (1941) Theory of Rate Processes. McGraw-Hill, New York

Gleason JF, Sinha A, Howard CJ (1987) Kinetics of the gas-phase $HOSO_2+O_2$ ->HO_2 +SO_3. J Phys Chem 91:719-724

Glidewell C, Thomson C (1984) *Ab initio* calculations on the effect of different basis-sets and electron correlation on the transition state for the reactions HNC reversible HCN and BCN reversible BNC. J Comput Chem 5:1-10

Glukhovtsev MN (1995) Should the standard basis-sets be augmented with diffuse functions on hydrogens to provide a reasonable description of the lowest Rydberg state of hydrogen-containing molecules. Theochem-J Mol Struc 357:237-242

Goedecker S (1999) Linear scaling electronic structure methods. Rev Mod Phys 71:1085-1123

Grüneich A, Hess BA (1998) Choosing GTO basis sets for periodic HF calculations. Theor Chem Acc 100:253-263

Hagfeldt A, Siegbahn H, Lindquist SE, Lunell S (1992) Semi-empirical calculations of TIO_2 (rutile) clusters. Int J Quantum Chem 44:477-495

Halasz GJ, Vibok A, Mayer I (1999) Comparison of basis set superposition error corrected perturbation theories for calculating intermolecular interaction energies. J Comput Chem 20:274-283

Halgren TA, Lipscomb WN (1977) The synchronous-transit method for determining reaction pathways and locating molecular transition states. Chem Phys Lett 49:225-232

Hammond GS (1955) A correlation of reaction rates. J Am Chem Soc 77:334-338

Harris D, Loew GH, Kormonicki A (1997) Structure and relative spin state energetics of $Fe(H_2O)_6^{3+}$: A comparison of UHF, Moller-Plesset, nonlocal DFT, and semiempirical INDO/S calculations. J Phys Chem A 101:3959-3965

Head JD, Zerner MC (1989) Newton based optimization methods for obtaining molecular-conformation. Adv Quantum Chem 20:239-290

Hehre WJ, Radom PR, Pople JA (1986) *Ab initio* Molecular Orbital Theory. Wiley Interscience, New York

Herzberg, G (1950) Molecular spectra and molecular structure. Van Nostrand, New York

High Performance Computational Chemistry Group (1998) NWChem, A Computational Chemistry Package for Parallel Computers, Version 3.3.1. Pacific Northwest National Laboratory, Richland, WA

Hirva P, Pakkanen TA (1992) The interaction of amine bases on the Lewis acid sites of aluminum-oxide - a theoretical-study. Surf Sci 277:389-394

Hofmann M, Schleyer PV (1994) Acid-rain—*ab initio* investigation of the $H_2O•SO_3$ complex and its conversion into H_2SO_4. J Am Chem Soc 116:4947-4952

Hohenberg P, Kohn W (1964) Inhomogeneous electron gas. Phys Rev B 136:864-871

Hynes JT (1985) The theory of reactions in solutions. *In:* Theory of Chemical Reaction Dynamics. Baer M (ed), CRC Press, Boca Raton, p 171-234

Ihinger, P (1991) An experimental study of the interaction of water with granitic melt. PhD dissert. California Institute of Technology. 190 pp

Jaguar v.3.5. (1998) Schrodinger Inc., Portland OR

Jitariu LC, Hirst DM (1998) An *ab initio* study of the singlet potential-energy surface for the reaction of NO_3 with HO_2. J Chem Soc Faraday T 94:1379-1384

Jitariu LC, Hirst DM (1999) *Ab initio* study of the reaction of NO_3 with the OH radical. J Phys Chem A 103:6673-6677

Johnson BG (1994) The performance of a family of density-functional methods. J Chem Phys 101:9202-9202

Johnston HS (1966) Gas phase reaction rate theory. Ronald Press, NY

Jones PD, Wigley TML, Wright PB (1986) Global temperature-variations between 1861 and 1984. Nature 322:430-434.

Jungwirth P (2000) How many waters are necessary to dissolve a rock salt molecule? J Phys Chem A 104:145-148

Kinrade SD, Del Nin JW, Schach AS, Sloan TA, Wilson KL, Knight CTG (1999) Stable five- and six-coordinated silicate anions in aqueous solution. Science, 285:1542-1545

Kohn W, Sham LJ (1965) Self-consistent equations including exchange and correlation effects. Phys Rev 140:1133-1140

Kolb CE, Jayne JT, Worsnop DR, Molina MJ, Meads RF, Viggiano AA (1994) Gas-phase reaction of sulfur-trioxide with water-vapor. J Am Chem Soc 116:10314-10315

Kubicki JD, Xiao Y, Lasaga AC (1993) Theoretical reaction pathways for the formation of $[Si(OH)_5]^{1-}$ and the deprotonation of orthosilicic acid in basic solution. Geochim Cosmochim Acta 57:3847-3863

Kubicki JD, Apitz SE, Blake GA (1995) G2 theory calculations on $[H_3SiO_4]^-$, $[H_4SiO_4]$, $[H_3AlO_4]^{2-}$, $[H_4A1O_4]^-$ and $[H_5AlO_4]$: Basis set and electron correlation effects on molecular structures, atomic charges, infrared spectra, and potential energies. Phys Chem Miner 22:481-488

Kubicki JD, Blake GA, Apitz SE (1996) *Ab initio* calculations on aluminosilicate Q(3) species: Implications for atomic structures of mineral surfaces and dissolution mechanisms of feldspars. Am Mineral 81:789-799

Kuroda Y, Hariya Y, Suzuoki T, Matsuo S (1982) D/H fractionation between water and the melts of quartz, K-feldspar, albite and anorthite at high temperature and pressure. Geochem J 16:73-78

Lasaga AC (1981) Transition state theory. *In:* Kinetics of Geochemical Processes. Lasaga AC, Kirkpatrick RJ (eds). Rev Mineral. Mineral Soc Am, Washington DC, 8:135-170

Lasaga AC (1992) *Ab initio* methods in mineral surface reactions. Rev Geophysics 30:269-303

Lasaga AC (1995) Fundamental approaches in describing mineral dissolution and precipitation rates. *In:* Chemical Weathering Rates of Silicate Minerals, White AF, Brantley SL (eds), Rev Mineral, Mineral Soc Am, Washington DC, 31:23-86

Lasaga AC (1998) Kinetic Theory in the Earth Sciences. Princeton University Press, Princeton, New Jersey

Lasaga AC, Gibbs GV (1990) *Ab initio* quantum mechanical calculations of water-rock interactions: adsorption and hydrolysis reactions. Am J Sci 290:263-295

Lasaga AC, Gibbs GV (1991) *Ab initio* studies of the kinetic isotope effect of the CH_4 + OH. atmospheric reaction. Geophys Res Lett 18:1217-1220

Leffler JE (1953) Parameters for the description of transition states. Science 117:340-341

Li WK, McKee ML (1997) Theoretical study of OH and H_2O addition to SO_2. J Phys Chem A 101:9778-9782

Liedl KR (1998) Dangers of counterpoise corrected hypersurfaces. Advantages of basis set superposition improvement. J Chem Phys 108:3199-3204

Lindblad M, Pakkanen TA (1993) Cluster-models for the interaction of HCl with nonpolar surfaces of gamma-Al_2O_3. Surf Sci 286:333-345

Lu X, Musin RN, Lin MC (2000) Gas-phase reactions of HONO with HNO and NH_3: an *ab initio* MO/TST study. J Phys Chem A 104:5141-5148

Majumdar D, Kim GS, Kim J, Oh KS, Lee JY, Kim KS, Choi WY, Lee SH, Kang MH, Mhin BJ (2000) *Ab initio* investigations on the $HOSO_2+O^{-2} \rightarrow SO_3+HO_2$ reaction. J Chem Phys 112:723-730

Manassidis I, Devita A, Gillan MJ (1993) Structure of the (0001) surface of α-Al_2O_3 from first principles calculations. Surf Sci 285:l517-l521

Mann ME, Park J (1996) Greenhouse warming and changes in the seasonal cycle of temperature: Model versus observations. Geophys Res Lett 23:1111-1114

Manthe U, Miller WH (1993) The cumulative reaction probability as eigenvalue problem. J Chem Phys 99:3411-3419

Margitan JJ (1984) Mechanism of the atmospheric oxidation of sulfur-dioxide—catalysis by hydroxyl radicals. J Phys Chem 88:3314-3318

Maroulis G (1998) Hyperpolarizability of H_2O revisited: accurate estimate of the basis set limit and the size of electron correlation effects. Chem Phys Lett 289:403-411

Martin JML, Francois JP, Gijbels R (1989) Combined bond-polarization basis-sets for accurate determination of dissociation-energies 2. Basis set superposition error as a function of the parent basis set. J Comput Chem 10:875-886

Martins JBL, Andres J, Longo E, Taft CA (1995) A theoretical-study of $(10\bar{1}0)$ and (0001) ZnO surfaces—molecular cluster model, basis-set and effective core potential dependence. Theochem-J Mol Struc 330:301-306

Matsumura K, Lovas FJ, Suenram RD (1989) The microwave-spectrum and structure of the H_2O-SO_2 complex. J Chem Phys 91:5887-5894

Mayer I (1983) Towards a chemical hamiltonian. Int J Quantum Chem 23:341-363.

McQuarrie DA (1973) Statistical Thermodynamics. University Science Books, California, 343 pp

Mebel AM, Morokuma K (1996) Theoretical study of the reaction of HCl with $ClONO_2$ catalyzed by NO_3^-. "Attachment-detachment" mechanism for the anion-catalyzed neutral reactions. J Phys Chem 100:2985-2992

Mebel AM, Lin MC, Melius CF (1998) Rate constant of the HONO+HONO → H_2O+NO+NO_2 reaction from *ab initio* MO and TST calculations. J Phys Chem A 102:1803-1807

Melissas VS, Truhlar DG (1993a) Deuterium and C-13 kinetic isotope effects for the reaction of OH with CH_4. J Chem Phys 99:3542-3552

Melissas VS, Truhlar DG (1993b) Interpolated variational transition state theory and tunneling calculations of the rate-constant of the reaction OH+CH_4 at 223-2400 K. J Chem Phys 99:1013-1027

Miertus S, Scrocco E, Tomasi J (1981) Electrostatic interaction of a solute with a continuum—a direct utilization of *ab initio* molecular potentials for the prevision of solvent effects. Chem Phys 55:117-129

Miller WH (1975) Semiclassical limit of quantum-mechanical transition state theory for nonseparable systems J Chem Phys 62:1899-1906

Miller WH (1993) Beyond transition state theory: A rigorous quantum theory of chemical reaction rates. Acc Chem Res 26:174-181

Miller WH (1998) Rates of chemical reactions. *In:* Encyclopedia of Computational Chemistry. Schleyer PVR, Allinger NL, Clark T, Gasteiger J, Kollman PA, Schaefer HF III, Schreiner PR (eds), Wiley, Chichester, NY, p 2375-2380

Moller C, Plesset MS (1934) Note on an approximation treatment for many-electron systems. Phys Rev 46:618-622

Morokuma K, Muguruma C (1994) *Ab initio* molecular orbital study of the mechanism of the gas-phase reaction SO_3+H_2O—importance of the 2nd water molecule. J Am Chem Soc 116:10316-10317

Mitin AV, Hirsch G, Buenker RJ (1996) Accurate small split-valence 3-21SP and 4-22SP basis sets for the first-row atoms. Chem Phys Lett 259:151-158

Muilu J, Pakkanen TA (1994) *Ab initio* models for ZnS surfaces—influence of cluster-size on surface-properties. Phys Rev B 49:11185-11190

Murrell JN, Farantos S (1977) Analytical function for potential-energy surface of ozone. Mol Phys 34:1185-1188

Murrell JN, Carter S, Farantos SC, Huxley P, Varandas AJC (1984) Molecular Potential Energy Functions. Wiley-Interscience. New York

Nath S, Nandi PK, Sannigrahi AB, Chattaraj PK (1993) Effect of basis-sets and population analysis schemes on the calculation of group electronegativity. Theochem-J Mol Struc 98:207-211

Nath S, Sannigrahi AB, Chattaraj PK (1994) Effect of basis-sets on *ab initio* SCF calculations of molecular hardness. Theochem-J Mol Struc 112:87-90

Nicholas JB, Winans RE, Harrison RJ, Iton LE, Curtiss LA, Hopfinger AJ (1992) *Ab initio* molecular-orbital study of the effects of basis set size on the calculated structure and acidity of hydroxyl-groups in framework molecular-sieves. J Phys Chem 96:10247-10257

Nortier P, Borosy AP, Allavena M (1997) *Ab initio* Hartree-Fock study of Bronsted acidity at the surface of oxides. J Phys Chem B 101:1347-1354

Ordejon P (1998) Order-N tight-binding methods for electronic-structure and molecular dynamics. Com Mater Sci 12:157-191

Orlando R, Dovesi R, Ugliengo P, (1999) A quantum mechanical periodic *ab initio* approach to materials science: the CRYSTAL program. Int J Inorg Mater 1:147-155

Oum KW, Lakin MJ, DeHaan DO, Brauers T, Finlayson-Pitts BJ (1998) Formation of molecular chlorine from the photolysis of ozone and aqueous sea-salt particles. Science 279:74-77

Paizs B, Suhai S (1997) Extension of SCF and DFT versions of chemical Hamiltonian approach to N interacting subsystems and an algorithm for their efficient implementation. J Comput Chem 18:694-701

Pan YP, McAllister MA (1998) Characterization of low-barrier hydrogen bonds 4. Basis set and correlation effects: an *ab initio* and DFT investigation. Theochem-J Mol Struc 427:221-227

Papadopoulos MG, Waite J (1991) The effect of basis set variation and correlation on the 2nd hyperpolarizability of H_20. Theochem-J Mol Struc 81:137-146

Pechukas P (1976) Statistical Approximations in collision theory. *In:* Dynamics of Molecular Collisions. Part B. Miller WH (ed), Plenum Press, New York, p 269-322

Pelmenschikov H, Strandh H, Pettersson, LGM, Leszczynski J (2000) Lattice resistance to hydrolysis of Si-O-Si bonds on silicate minerals: *Ab initio* calculations of a single water attack onto the (001) and (111) β-cristobalite surfaces. J Phys Chem B ASAP Article.

Peng C, Ayala PY, Schlegel HB, Frisch MJ, (1996) Using redundant internal coordinates to optimize geometries and transition states. J Comp Chem 17:49-56

Peng C, Schlegel HB (1994) Combining synchronous transit and quasi-newton methods for finding transition states. Israel J Chem 33:449-454

Pereira JCG, Catlow CRA, Price GD (1999) *Ab initio* studies of silica-based clusters. Part I. Energies and conformations of simple clusters. J Phys Chem A 103:3252-3267

Pisani C, Dovesi R (1980) Exact-exchange Hartree-Fock calculations for periodic systems. I. Illustration of the method. Int J Quantum Chem 17:501-516

Pisani C, Ricca F (1980) Embedded versus non-embedded-cluster treatment of chemisorbed systems—model computation. Surf Sci 92:481-488

Pisani C, Dovesi R, Roetti C (1988) Hartree-Fock *ab initio* of crystalline systems, Lecture Notes in Chemistry, Vol. 48, Spinger Verlag, Heidelberg

Pisani C, Dovesi R, Roetti C, Causa M, Orlando R, Casassa S, Saunders VR (2000) CRYSTAL and EMBED, two computational tools for the *ab initio* study of electronic properties of crystals. Int J Quantum Chem 77:1032-1048

Pommerening CA, Bachrach SM, Sunderlin LS (1999) Addition of protonated water to SO_3. J Phys Chem A 103:1214-1220

Press WH, Teukolsky SA, Vetterling WT, Flannery BP (1992) Numerical Recipes in C, 2nd ed. Cambridge University Press, New York

Pulay P, Fogarasi G, Pang F, Boggs JE (1979) Systematic *ab initio* gradient calculation of molecular geometries, force constants, and dipole-moment derivatives. J Am Chem Soc 101:2550-2560

Pulay P, Fogarasi G (1992) Geometry optimization in redundant internal coordinates. J Chem Phys 96:2856-2860

Rosso KM, Gibbs GV, Boisen MB (1999) SiO bonded interactions in coesite: a comparison of crystalline, molecular and experimental electron density distributions. Phys Chem Min 26:264-272

Rubio J, Russo N, Sicilia E (1997) Density functional potential energy hypersurface of protonated ozone: A comparison between different gradient-corrected nonlocal functionals. Int J Quantum Chem 61:415-420

Rust F, Stevens CM (1980) Carbon kinetic isotope effect in the oxidation of methane by hydroxyl. Int J Chem Kinet 12:371-377

Saebo S, Tong W, Pulay P (1993) Efficient elimination of basis set superposition errors by the local correlation method—accurate *ab initio* studies of the water dimer. J Chem Phys 98:2170-2175

Saunders VR (1984) *Ab initio* Hartree-Fock Calculations for periodic systems. Faraday Symp. Chem. Soc. 19:79-84

Schaefer HF (1972) The electronic structure of atoms and molecules; a survey of rigorous quantum mechanical results. Addison-Wesley, Massachusetts

Schlegel HB (1987) Optimization of equilibrium geometries and transition structures. Adv Chem Phys 67:249-286

Schlegel HB (1982) Optimization of equilibrium geometries and transition structures. J Comp Chem 3:214-218

Schmidt MW, Baldridge KK, Boatz JA, Elbert ST, Gordon MS, Jensen JH, Koseki S, Matsunaga N, Nguyen KA, Su S, Windus TL, Dupuis M, Montgomery JA (1993) General atomic and molecular electronic structure system. J Comput Chem 14:1347-1363

Schoeberl MR, Hartmann DL (1991) The dynamics of the stratospheric polar vortex and its relation to springtime ozone depletions. Science 251:46-52

Schoell M (1980) The hydrogen and carbon isotopic composition of methane from natural gases of various origins. Geochim Cosmochim Acta 44:649-661

Schriver L, Carrere D, Schriver A, Jaeger K (1991) Matrix-isolation photolysis of SO_2, O_3 AND H_2O—evidence for the H_2O-SO_3 complex. Chem Phys Lett 181:505-511

Schultz PA, Stechel EB (1998) Effects of basis set quality on the prediction of structures, energies, and properties of amorphous tetrahedral carbon. Phys Rev B 57:3295-3304

Seideman T, Miller WH (1992) Calculation of the cumulative reaction probability via a discrete variable representation with absorbing boundary-conditions. J Chem Phys 96:4412-4422

Seideman T, Miller WH (1993) Quantum-mechanical reaction probabilities via a discrete variable representation-absorbing boundary-condition green-function. J Chem Phys 97:2499-2514

Sierka M, Sauer J (2000) Finding transition structures in extended systems: A strategy based on a combined quantum mechanics-empirical valence bond approach. J Chem Phys 112:6983-6996

Simon S, Duran M, Dannenberg JJ (1999) Effect of basis set superposition error on the water dimer surface calculated at Hartree-Fock, Moller-Plesset, and density functional theory levels. J Phys Chem A 103:1640-1643

Simon S, Duran M, Dannenberg JJ (1996) How does basis set superposition error change the potential surfaces for hydrogen bonded dimers? J Chem Phys 105:11024-11031

Smith BJ, Radom L (1995) Gas-phase acidities—a comparison of density-functional, MP2, MP4, F4, G2(MP2, SVP), G2(MP2) and G2 procedures. Chem Phys Lett 245:123-128

Sordo JA (2000) On the important role played by polarization functions in calculations involving hypervalent molecules. Chem Phys Lett 316:167-170

Stevens CM, Engelkemeir A (1988) Stable carbon isotopic composition of methane from some natural and anthropogenic sources. J Geophys Res-Atmos 93:725-733

Stewart JJR (1993) MOPAC93. QCPE Program Number: 689

Tanaka N, Rye DM, Xiao Y, Lasaga AC (1994) Use of stable sulfur isotope systematics for evaluating oxidation reaction pathways and in-cloud scavenging of sulfur-dioxide in the atmosphere. Geophys Res Lett 21:1519-1522

Thompson WH, Miller WH (1995) On the direct calculation of thermal rate constants. J Chem Phys 102:7409-7417

Tossell JA, Vaughan DJ (1992) Theoretical Geochemistry: Applications of Quantum Mechanics in the Earth and Mineral Sciences. Oxford University Press, Oxford

Truhlar DG, Garrett BC, Klippenstein SJ (1996) Current status of transition state theory. J Phys Chem 100:12771-12800

Truhlar DG, Hase WL, Hynes JT (1983) Current status of transition state theory. J Phys Chem 87:2664-2682

Truhlar DG, Isaacson AD, Garrett BC (1985) Generalized transition state theory. *In:* Theory of Chemical Reaction Dynamics. Baer M (ed), CRC Press, Boca Raton, p 65-137

Truhlar DG, Isaacson AD, Skodje RT, Garrett BC (1982) Incorporation of quantum effects in generalized-transition state theory. J Phys Chem 86:2252-2261

Truong TN, Truhlar DG (1990) *Ab initio* transition state theory calculations of the reaction-rate for $OH+CH_4->H_2O+CH_3$. J Chem Phys 93:1761-1769

Tschumper GS, Kelty MD, Schaefer HF (1999) Subtle basis set effects on hydrogen bonded systems. Mol Phys 96:493-504

Tsuzuki S, Uchimaru T, Tanabe K (1994) Basis-set effects on the intermolecular interaction of hydrocarbon molecules obtained by an *ab initio* molecular-orbital method—evaluation of dispersion energy. Theochem-J Mol Struc 113:107-118

Tsuzuki S, Uchimaru T, Tanabe K. Yliniemela A (1996) Comparison of atomic charge distributions obtained from different procedures: Basis set and electron correlation effects. Theochem-J Mol Struc 365:81-88.

Tsuzuki S, Uchimaru T, Matsumura K, Mikami M, Tanabe K (1999) Effects of basis set and electron correlation on the calculated interaction energies of hydrogen bonding complexes: MP2/cc-pV5Z calculations of H_2O-MeOH, H_2O-Me_2O, H_2O-H_2CO, MeOH-MeOH, and HCOOH-HCOOH complexes. J Chem Phys 110:11906-11910

Turekian KK (1996) Global Environmental Change. Prentice-Hall, New Jersey

Turi L, Dannenberg JJ (1993) Correcting for basis set superposition error in aggregates containing more than 2 molecules - ambiguities in the calculation of the counterpoise correction. J Phys Chem 97:2488-2490

Tyler SC (1992) Kinetic isotope effects and their use in studying atmospheric trace species case-study, CH_4+OH. ACS Sym Ser 502:390-408

Valiron P, Vibok A, Mayer I (1993) Comparison of a posteriori and a priori BSSE correction schemes for SCF intermolecular energies. J Comput Chem 14:401-409

van Duijneveldt FB (1997) From van der waals to strongly bound complexes. *In:* Scheiner S (ed) Molecular Interactions: Wiley, New York

Vincent MA, Palmer IJ, Hillier IH (1997) An *ab initio* study of the structure and energetics of the bisulfite ion in the gas phase and in aqueous solution. Theochem-J Mol Struc 394:1-9

Werner HJ, Knowles PJ (1999) MOLPRO version 2000.1, University of Birmingham, UK

Wong MW, Frisch MJ, Wiberg KB (1991) Solvent effects 1. The mediation of electrostatic effects by solvents. J Am Chem Soc 113:4776-4782

Xantheas SS (1995) *Ab initio* studies of cyclic water clusters $(H_2O)(n)$, n=1-6 3. Comparison of density-functional with MP2 results. J Chem Phys 102:4505-4517

Xantheas SS, Atchity GJ, Elbert ST, Ruedenberg K (1991) Potential-energy surfaces of ozone. J Chem Phys 94:8054-8069

Xenides D, Maroulis G (2000) Basis set and electron correlation effects on the first and second static hyperpolarizability of SO_2. Chem Phys Lett 319:618-624

Xiao Y, Lasaga AC (1994) *Ab initio* quantum mechanical studies of the kinetics and mechanisms of quartz dissolution: H^+/H_3O^+ catalysis. Geochim Cosmochim Acta 58:5379-5400

Xiao Y, Lasaga AC (1996) *Ab initio* quantum mechanical studies of the kinetics and mechanisms of quartz dissolution: OH^- catalysis. Geochim Cosmochim Acta 60:2283-2295

Xu SC, Zhao XS (1999) Theoretical investigation of the reaction of $ClONO_2$ with H_2O on water clusters. J Phys Chem A 103:2100-2106

Zhang JZH, Miller WH (1989) Quantum reactive scattering via the S-matrix version of the Kohn variational principle—differential and integral cross-sections for $D+H_2 \rightarrow HD+H$. J Chem Phys 91:1528-1547